P2

Final Report

F73-04

CIT Photoheliograph
Functional Verification Unit Test Program
Phase 2

Prepared for:

NATIONAL AERONAUTICS AND SPACE ADMINISTRATION
George C. Marshall Space Flight Center
Huntsville, Alabama

Contract No. NAS 8-29151

June 1973

BALL BROTHERS RESEARCH CORPORATION
SUBSIDIARY OF BALL CORPORATION
BOULDER, COLORADO

CIT PHOTOHELIOGRAPH
FUNCTIONAL VERIFICATION UNIT TEST PROGRAM
PHASE 2

Final Report
F73-04

Prepared for:
NATIONAL AERONAUTICS AND SPACE ADMINISTRATION
George C. Marshall Space Flight Center
Huntsville, Alabama

Contract No. NAS 8-29151
June 1973

FOREWORD

The CIT Photoheliograph test program was performed for NASA/MSFC under Contract NAS 8-29151. This final report describes the Phase 2 tests and their results. Phase 1 tests were reported in Ball Brothers Research Corporation final report No. F72-04.

Ball Brothers Research Corporation personnel who worked on this program included the following:

J. Roach	Program Manager
A. Olsen	Project Engineer
A. Frank, J. Tedesco, W. Nelson, E. Dereniak	System Testing
B. Weller, E. Worner	Data Analysis

NASA/MSFC personnel contributing to this program were the following:

Max Nein	PD-MP-A
Charles Wyman	S&E-ASTR-RP
Keith Clark	S&E-ASTR-GCI
Greg Sensmeier	S&E-ASTR-GCI

Mr. Nein was responsible for technical direction on the contract; Mr. Wyman acted as an optical test consultant; and Messrs. Clark and Sensmeier conducted floor stability tests (see Appendix C) to establish that the test site would be satisfactory.

Professor Robert R. Shannon, Optical Science Center, University of Arizona, acted as consultant to BBRC during all phases of the program.

SUMMARY

Tests of the 2/3-meter Photoheliograph FVU (Functional Verification Unit) were performed with the FVU installed in its Big Bear Solar Observatory vacuum chamber. Interferometric tests were run both in Newtonian (f/3.85) and Gregorian (f/50) configurations. Tests were run in both configurations with optical axis horizontal, vertical, and at 45° to attempt to determine any gravity effects on the system. Gravity effects, if present, were masked by scatter in the data associated with the system wavefront error of 0.16 λ rms (λ = 6328Å) apparently due to problems in the primary mirror. Tests showed that the redesigned secondary mirror assembly works well.

CONTENTS

APPENDICES

ILLUSTRATION

TABLES

Section 1
INTRODUCTION

Objectives of this test program were:

- To check for gravity effects, both in the figure of the primary mirror and in the pointing of the entire telescope.
- To check the general operation and image quality of the FVU before shipment to Big Bear.
- To check out the newly-designed secondary positioning mechanism and the alignment-sensing system.

As is usual with development test programs, the surprises during testing outweighed the original objectives and forced changes in the original test plans. Checking for gravity effects on the primary mirror figure, to the precision desired, required an extremely sensitive and stable test method and setup. The extremely short original schedule (twelve weeks) forced us to plan and build all of the fixturing simultaneously, and to design it to match the anticipated precision required in the gravity tests.

In retrospect, this was unnecessary. The primary mirror proved to have a large figure error, and this error precluded precise analysis of the changes due to gravity.

This program also interlocked with other Photoheliograph-oriented programs. It came near the end of the task of redesigning and fabricating a new secondary mirror assembly. It used as fixturing a vacuum chamber built by BBRC for use at Big Bear Solar Observatory. It required close coordination with Tinsley Laboratories, under

separate contract with MSFC to mount and test the test flat, and then deliver it to BBRC for use in our test setup.

In Section 2 we will briefly describe the test methods used. In Section 3 we present and discuss the test results.

Details of test equipment, and data-reduction methods are in Appendices A, B and C.

Section 2
TEST METHODS

2.1 ORDER OF TESTS

The Photoheliograph FVU is a Gregorian telescope with two additional folding mirrors and a heat-stop mirror. Primary-to-secondary alignment and focus are quite critical, hence the secondary is adjustable remotely by means of three actuators, which drive it in translation and tilt (not in focus) as sensed by an auxiliary system which includes a laser-diode projector at the secondary, and an optical sensor at the primary.

The general order of events in the test was as follows:

- Install and align the primary, secondary, and alignment system components.
- Install an auxiliary Newtonian flat between primary and secondary.
- Install the FVU in its vacuum chamber.
- Test the primary mirror in the f/3.85 Newtonian configuration, using the MSFC test flat in autocollimation.
- Remove the Newtonian flat, install the second folding mirror, and test the entire FVU at f/50, using the MSFC test flat in autocollimation.

Sections which follow give more details on the above.

2.2 INITIAL ALIGNMENT

The FVU was optically aligned while in a BBRC optical laboratory. Alignment was done with the instrument in a horizontal position on a granite slab.

The basic steps were:

1. Locate the center of curvature of the primary mirror. This was done using the Ann Arbor Tester in a knife edge fashion. Once this was done, a set of cross hairs was placed temporarily at the axial radius of curvature of the primary. See sketch below.

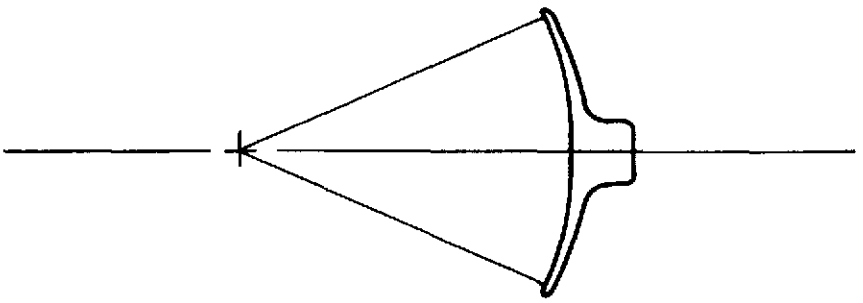

This established one point on the optical axis.

2. A set of cross hairs in a centering plug in the primary mirror was used to locate another point on the optical axis.

3. A Davidson Autocollimating Telescope was mounted behind the telescope primary and boresighted to lie in line with the center of the primary and its radius of curvature. This established the optical axis of the primary.

4. The secondary mirror was aligned inside the secondary housing by moving it until the center of its field (as defined by best imagery) was centered in the hole in the heat-stop mirror. In this setup, a multiple star source (a front-illuminated piece of opaque adhesive tape) was used at the long conjugate, and its image observed with a microscope at the short conjugate.

5. The spider and secondary housing were then mounted and aligned to the optical axis using the autocollimator as the reference. Coarse alignment was determined by focusing the autocollimator on the hole in the heat stop mirror and translating the entire pod until the field stop was centered.

6. The longitudinal position and tilt of the secondary housing were established using the LUPI as a reimaging microscope at the f/50 focus. See sketch below. This established the Z position by linear measurement from the diagonal mirror.

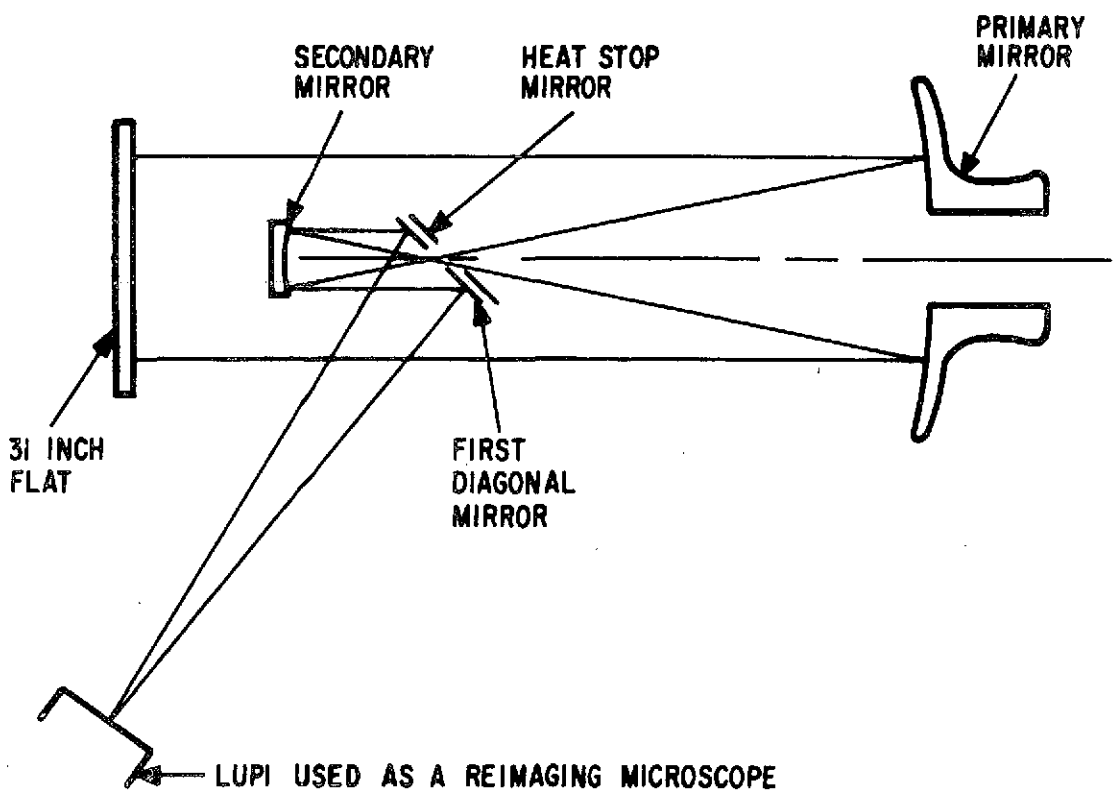

2.3 PRIMARY MIRROR TESTS (f/3.85)

Following initial alignment of the FVU a Cer-Vit Newtonian flat, 9.4 x 6.6 x 1.7 inches, was mounted to an auxiliary frame between the primary and its prime focus, as shown in Figure A-3 (Appendix A). This flat was aligned to put the focal point of the primary at the calculated focal point of the LUPI diverger lens when mounted in the vacuum chamber. The LUPI diverger was mounted inside the chamber during these tests, so that the vacuum chamber window would be in the collimated space between LUPI and diverger. Having the window in the f/3.85 space between diverger and primary would have caused serious spherical aberration, complicating system alignment.

The FVU was then moved to a high bay area where a 10-ton overhead hoist was available. This hoist was used to lower the FVU into the open end of the vacuum chamber, which was set with its long axis vertical. The vacuum chamber was then tilted to horizontal and towed on its wagon to the approved test site (See Appendix C).

The main test was to be evaluation of the figure of the primary mirror under three different orientations of gravity: 0° (horizontal), 45°, and 90°. Since the expected changes were extremely small, the test setup was done with the FVU in vacuum, to prevent optical problems from air currents in the light path. The entire chamber and the wagon on which it was transported were mounted on Barry Controls pneumatic supports to attenuate vibration transmitted from the floor.

With the chamber horizontal, the LUPI was used to obtain interferograms in the optical setup shown in Figure A-3 (Appendix A). These interferograms showed the figure problems of the primary mirror, although they could not be separated at this point from possible errors in the MSFC flat or the Newtonian flat. It was decided, in part because of the extremely tight schedule, to proceed with 45° and 90° tests to try to find any further system problems. Interferograms were duly taken at 45° and 90°. However, a fixturing difficulty required turning the end plate of the vacuum chamber 30°, in its own plane (i.e., 30° around the perpendicular to its face) and with it the MSFC flat, which was mounted to it. Since the interferograms represent the sum of the errors of the primary and the test optics, figure defects due to the flat would appear in the interferograms. If these were not rotationally symmetric about the center of the flat, they would affect the interferograms differently before and after rotation. However, the errors of the MSFC flat turned out to be small compared to those of the primary, hence the rotation caused no problem.

The chamber was then returned to 0°. There were large motions of the return image as the chamber was tilted. These motions could have been caused by motion (relative to the chamber) of the primary mirror, the entire FVU, or the MSFC flat. The problem turned out to be in the articulated mount for the flat, which allowed undue flexure under the load of the flat and its cell. After the chamber was returned to 0°, the mount for the flat was disassembled and strengthened sufficiently to alleviate the problem greatly. At the same time, at the suggestion of Mr. Richard Prout of CIT, the MSFC flat was remounted in a three-point manner to prevent any possible distortion from the mounting plate.

Final pictures at 0° were taken after these changes to the mount.

2.4 SYSTEM TESTS (f/50)

Following the f/3.85 tests, the FVU, chamber and wagon were towed back to the high bay area for setup in the f/50 test configuration. This included:

- Removal of the Newtonian flat and its mount. The Newtonian was left in its cell for possible future tests as mounted.*
- Going vertical with the chamber and hoisting the FVU and its mounting frame to a new position several inches forward of its "f/3.85" position. The f/3.85 mounting position was used to permit use of an existing port in the BBSO chamber for the test involving the Newtonian flat.
- Installation and alignment of the second fold mirror assembly (furnished by CIT).
- Installing the chamber feedthrough connectors for the alignment system.

Following these steps, the test rig was again moved to the approved test site and set up on the Barry mounts.

After some realignment work in the new configuration, and after rotating the MSFC flat 90°, it became apparent that the image problems really were in the primary mirror. At this point, we checked for possible mechanical reasons for the poor figure of

* These were subsequently done at CIT, and the mirror figure was reported to be good.

the primary, checking for mechanical interference behind the mirror, tightening and loosening the alignment sensor anchor bolt (which passes through the center of the mirror hub), removing a thermocouple from the back of the primary - and finding no change. From this point on, although some interferograms were taken and reduced, we realized that rework of the primary was necessary, and would be the eventual course of action. Subsequent tests (interferograms at 0°, 45° and 90° chamber position, and alignment system sensitivity checks) were run to make sure all systems worked well for future operation at BBSO.

These last tests were run with a plane-parallel tilted plate in the f/50 beam. As expected, this reduced the astigmatism, but did not produce enough improvement (the plate was of insufficient thickness) to cancel the astigmatism completely. In any event, the residual wavefront error even after removing astigmatism completely in the data reduction computer program was still excessive.

The brief alignment sensor checks showed that the alignment sensor was indeed sensitive to secondary pod motion with scale factors of about 4 mv/0.001 inch and 8 mv/0.001 inch in the two axes of translation. The channels were not zeroed, however, so the data is not representative of a properly adjusted system. We believe the alignment sensor was misaligned when its anchor rod was loosened, and should be realigned after the tests at CIT. The data also show from 0.1 to 0.2 mm of backlash (referred to the lateral position of the secondary) in each of the motor drives. The practical consequence is that the alignment system must be used to determine secondary pod position; merely counting pulses to the stepper-type drive motors is not sufficiently accurate.

3.0 TEST RESULTS AND DISCUSSION

Data from the 34 representative interferograms which were computer-reduced are summarized in Table 3-1. In each case, interferogram pairs are taken at exactly the same alignment of telescope, LUPI, and auxiliary optics: only the tilt of the reference beam (within the LUPI) is changed, to change the orientation of the fringes. Reduced data from pairs of interferograms is not identical, for data-sampling reasons (covered further in Appendix B). Different pairs taken under the same apparent conditions ordinarily differ in details of telescope or interferometer alignment.

In all cases, computer data are given for the wavefront exiting the entire system. This wavefront has gone from the LUPI through the telescope and any auxiliary optics such as the chamber window, Newtonian flat, etc., out to the MSFC flat, and return. Thus the wavefront has passed through the telescope twice, and the results tabulated must be divided by approximately two to express the results conventionally. These results will be only approximate because errors of the auxiliary optics, while markedly smaller than those of the FVU, also enter the results. These additional errors may either add or subtract from the data, since they may either increase or compensate for the errors of the FVU wavefront.

The "residual error" columns give the resultant error *after subtraction* from the wavefront of the aberration named. Thus, the "residual error-coma" column includes *no* comatic error component, but is the wavefront error after coma removal. The "no focus" column includes only the correction for wavefront tilt (which is intentionally introduced to produce fringes). The "focus" column has been corrected for focal errors, which are produced by position errors between the FVU and the LUPI.

Table 3-1

Photoheliograph Interferogram Data

Picture #	Fringe Orientation	Gravity Direction	Residual Error, Waves RMS: No Focus	Focus	Coma	Astig	Astig/Coma	Coma, Waves	Astig, Waves	
209	–	0° (Axis Horizontal)	.486	.412	.401	.299	.291	1.07	1.71	Ambient Pressure
210	|		.379		.359		.208	.36		
211	–		.427		.389		.248	.47		
212	|		.372	.357	.349	.211	.201	.76	1.59	
213	–		.408		.371		.188	.52		
214	|		.474	.430	.420	.327	.316	1.08	1.64	
215	–		.370	.350	.344	.218	.206	.80	1.57	
216	|		.382	.352	.336	.222	.213	1.21	1.62	
255	|	45°	.396	.340	.328	.201	.178	1.05	1.59	
256	–		.388	.348	.336	.210	.196	.92	1.46	
265	|		.462	.378	.374	.189	.187	.68	1.94	Telescope was double-passed by test wavefront. Results should be divided by approximately two (see text).
266	|		.396	.349	.343	.182	.174	.76	1.68	
267	–		.461	.427	.415	.224	.206	1.20	2.05	
287	–	90°	.329	.288	.264	.239	.208	1.05	.80	
288	|		.261	.242	.214	.187	.133	1.00	1.00	
289	–		.354	.293	.274	.211	.194	1.11	1.11	
290	|		.289	.262	.196	.216	.153	1.90	.92	
299	–	0°	.310	.287	.274	.189	.172	1.00	1.28	
300	|		.410	.375	.353	.224	.195	1.45	1.82	
301	|		.464	.457	.451	.215	.203	.77	2.10	- Avg of three digitizations
302	–		.417	.416	.407	.214	.194	.96	1.90	- Avg of three digitizations
330	|	0°	.480	.402	.390	.236	.184	1.07	2.00	f/50 With astigmatism-compensating tilt plate
331	–		.396	.350	.293	.221	.166	2.44	1.76	
340	|		.306	.290	.242	.261	.204	1.65	0.71	
341	–		.315	.304	.248	.266	.190	2.00	0.88	
355	–		.331	.330	.249	.256	.183	2.28	1.20	
356	|		.297	.297	.267	.242	.202	1.65	1.11	
358	–	45°	.378	.315	.270	.261	.156	1.60	1.47	
359	|		.362	.335	.296	.234	.150	1.49	1.36	
360	–	90°	.342	.341	.319	.221	.160	1.19	1.45	
361	|		.391	.387	.343	.238		1.75	1.61	
364	|	0°	.351	.344	.311	.249	.206	1.50	1.26	
365	–		.352	.339	.291	.238	.181	1.60	1.31	

There is a practical difference between coma and astigmatism in our tests in that coma is very sensitive to field position and astigmatism is not. Coma varies linearly with field, and astigmatism varies quadratically, as sketched below.

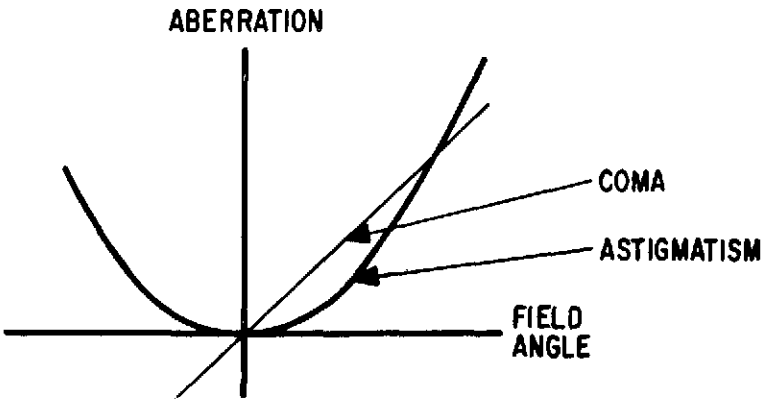

Thus for small field angles (such as during these tests) the component of astigmatism which changes with field position is negligible. Any astigmatism which is seen is attributable to fixed figure errors in system components, and not to alignment errors.

With coma, the situation is different. Since coma changes rapidly with field angle, any coma errors in the figures of the components can be compensated by moving to the proper field point.

Because of this difference it is proper to subtract any residual coma (but *not* astigmatism) in the computer, since with additional time and effort the coma could have been eliminated by realigning the system. For this reason the "coma" column in Table 3-1 is the most meaningful place to assess the quality of the optics. While there is a great deal of scatter in the data, the average "coma" residual of pictures 209 through 302 (the f/3.85 interferogram) is 0.33 λ rms. Pictures 330-331 (at f/50) average 0.34 λ rms, so the quality of the complete telescope is about the same as that of the primary. Thus, barring extreme coincidence, the components

which were different in the two test setups (LUPI diverger lens, Newtonian flat, secondary mirror and two folding mirrors) have errors very small compared to 0.33 λ rms.

The only components common to both setups are the primary and the MSFC flat. Test data on the flat is shown in Table 3-2, and surface maps are shown in Appendix A. Only five of the 28 test pictures supplied by Tinsley were reduced, since it was apparent that the flat was producing an insignificant part of the observed error. The average residual error after correcting for focus is 0.09 λ rms. This must be divided by two, since the flat was double-passed in these tests. Assuming this to be a random wavefront error, and noting that the primary mirror is double-passed in the BBRC tests, we have

$$\varepsilon_T^2 = (2\varepsilon_p)^2 + \varepsilon_T^2$$

where ε_T = computed residual after coma removal in BBRC tests

ε_p = wavefront error produced by single-passed primary

ε_F = wavefront error produced by single-passed test flat

or

$$\varepsilon_p = \frac{\sqrt{\varepsilon_T^2 - \varepsilon_F^2}}{2}$$

For ε_T = 0.33 λ rms and ε_F = 0.045 λ rms, ε_p = 0.164 λ rms.

Since this is about half of 0.33 λ (the half comes from single vs. double passing the primary), the error produced by the flat is negligible.

Table 3-2
MSFC FLAT INTERFEROGRAM DATA

Picture	Residual Error, Waves RMS No Focus	Focus	Astig.	Astig. Waves	
914	.077	.077	.052	.33*	Flat facing 45° up.
917	.098	.098		**	
918	.114	.112	.051	.58**	
922	.098	.092	.040	.53*	Surface of flat in vertical plane.
923	.085	.082	.037	.47*	

* Lower half of flat.
**Upper half of flat.

The data do not include contributions from a rather severe (~1 λ peak) turned-down edge on the primary. Personnel digitizing the interferograms did not scan the edge, since small differences in fringe position and orientation would have randomized the data unduly by adding a few data points with large deviations.

The 0.16 λ rms is much greater than the 0.074 λ rms allowed by Marechal's criterion (which would be equivalent to a 20 percent reduction in the Strehl Definition, and approximately equal to Rayleigh's $\frac{\lambda}{4}$ criterion for a "diffraction limited" telescope; see O'Neill, Introduction to Statistical Optics, Addison-Wesley, 1963).

Is 0.16 λ rms too large an error? As with most exercises involving the setting of tolerances, there is some intuition in the answer, but the following argument is of interest. Shannon has published (in Optical Instruments and Techniques, 1969, Ed. J. Home Dickson) calculated averaged MTF curves for varying amounts of rms random wavefront error. These were calculated for a particular random wavefront. The averaging is done over azimuth (that is, the direction--horizontal, vertical, or intermediate--of the bar pattern hypothetically being imaged by the system). If we assume a detection threshold at 5 percent image modulation (i.e., the image modulation must be at least 5 percent for the image feature to be detectable), then assume various values for target contrast, we can determine the "limiting resolution" as a function of rms random wavefront errors. Results are plotted in Figure 3-1 with target contrast as a parameter. The vertical coordinate is the normalized limiting resolution, where

$$S_o = \frac{1}{\lambda f/No} \text{ in line pairs per millimeter.}$$

The results of this exercise indicate that the 0.16 λ rms would cause little difficulty for high contrast targets; for a 100 percent contrast target the limiting spatial frequency has dropped only 15 percent, equivalent to a perfect telescope of 15 percent smaller diameter. For a target contrast of 10 percent, on the other hand, the loss is an intolerable 82 percent in limiting spatial frequency. In fact, for such low contrast it appears that even the Marechal criterion, giving a 36 percent drop, might not be sufficiently stringent.

In any event, for low and medium contrast targets the drop in limiting spatial frequency appears intolerable for a wavefront error of 0.16 λ rms.

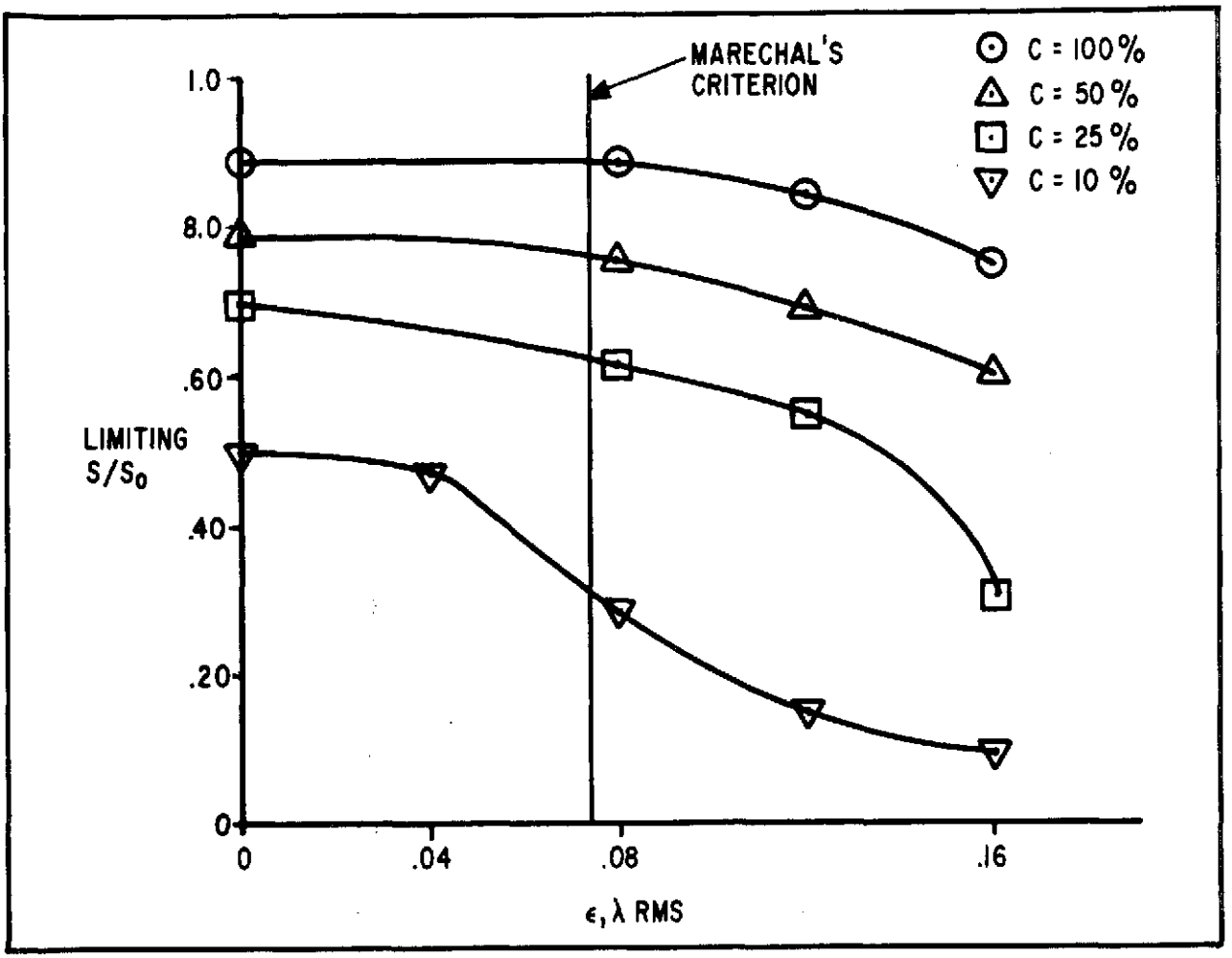

Figure 3-1 Limiting Resolution vs. rms Wavefront Error for Varying Target Contrast

The wavefront error in the primary mirror figure was possibly due to machining and acid etching processes performed on the primary mirror after figuring. Therefore, we recommend that the gravity effects tests be repeated after the primary mirror figure has been improved.

We conclude:

- The wavefront error produced by the photoheliograph in a single pass is about 0.16 λ rms at λ = 6328 Å. This error is not acceptable for low contrast targets.

- Virtually all of this wavefront error is caused by the primary mirror.

- Gravity effects, if present, were masked by scatter of the data due to the wavefront error.

- No sizable errors were caused by the test setup.

Appendix A
EQUIPMENT AND FACILITIES

Equipment and facilities required for testing of the FVU includes the vacuum chamber shown in Figures A-1 and A-2. This chamber was built under separate contract to house the FVU at Big Bear Solar Observatory (BBSO). A vacuum chamber was required, during tests, to prevent thermal and random air currents from disturbing the interferometry. The vacuum chamber was to be oriented variously with respect to gravity, and at the same time to be used for this extremely precise optical testing. Several ways of tilting the vacuum chamber were conceived and discarded because they required a strong overhead crane during use. BBRC has such a crane in the Integration and Test (I & T) Building, but this area is ruled out for precision interferometry because of high vibration and noise levels. An available area in another building (see Appendix C) was sufficiently quiet, but without needed hoist and headroom. Mounting the vacuum chamber on a BBRC four-wheel tilt fixture solved the problem. The crane handling work was done using the I & T Building crane (see Figure A-3), then the fixture, bearing the FVU in its vacuum chamber, rolled on its pneumatic tires to the approved test site, where the actual tilting and testing were done.

At BBSO the end plate shown in Figure A-2 will be replaced by one bearing a large window, through which the FVU will view the sun. The chamber will be mounted on an existing telescope fork.

Also visible in Figure A-2 is the Rootes-type pump, which pumped the chamber to pressures of a few tens of microns of mercury. This chamber was sealed off and the pump line was disconnected during actual tests, which were ordinarily run at pressures of less than one millimeter of mercury.

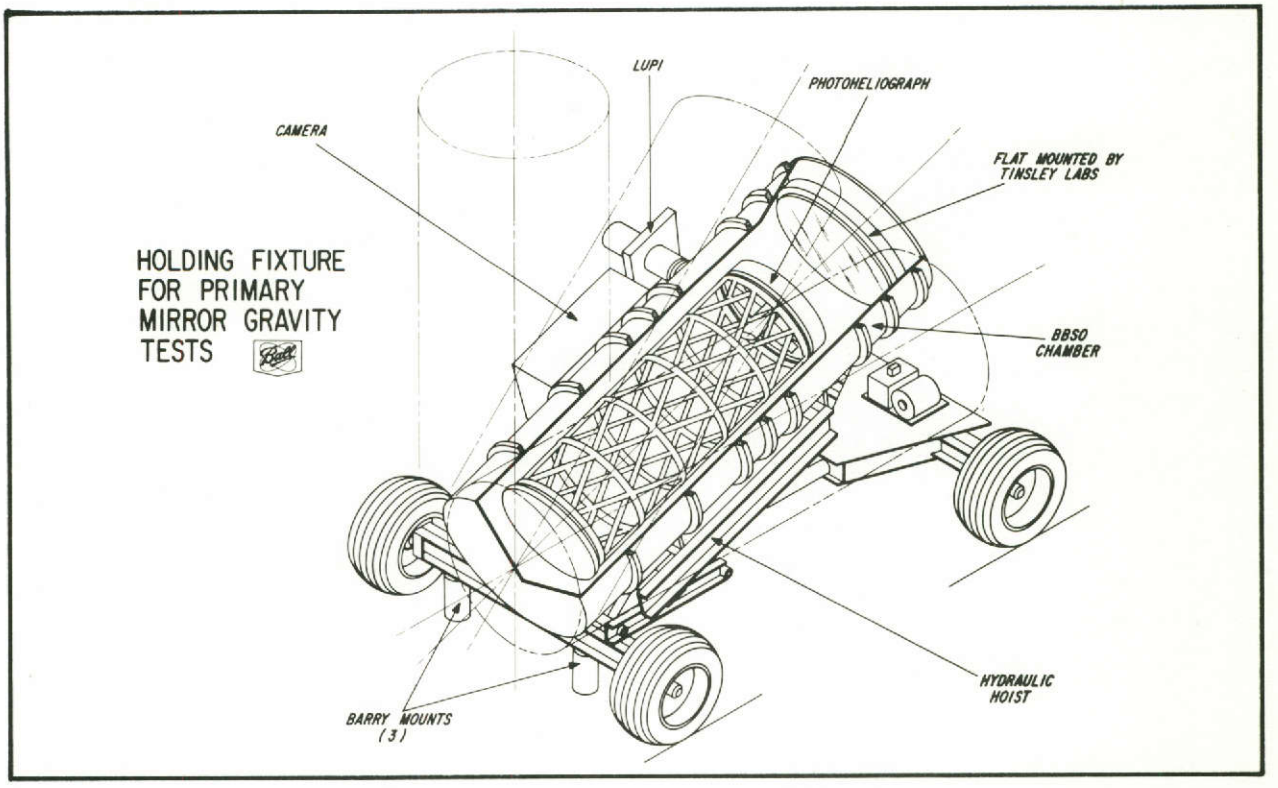

Figure A-1 Holding Fixture for Primary Mirror Gravity Tests

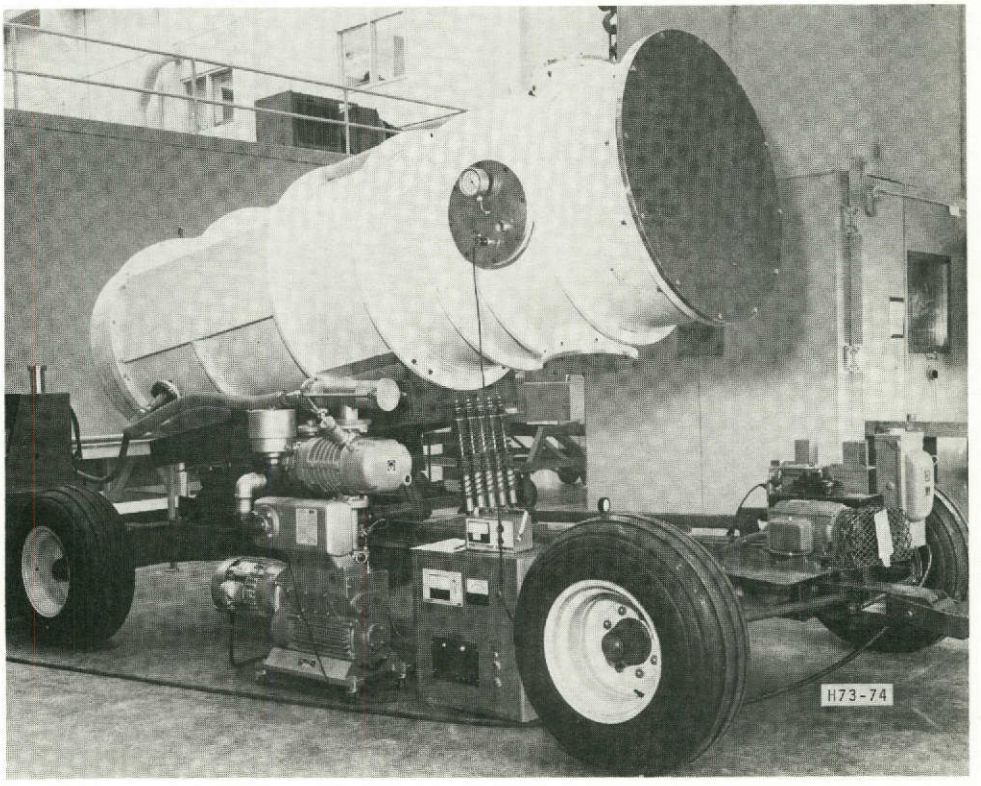

Figure A-2 PHG Chamber in Tilt Mode

During interferometric tests the entire wheeled tilt fixture was mounted on Barry Controls air mounts, which helped to attenuate ground-borne vibration.

Figures A-4 and A-5 depict the nominal configurations during f/3.85 and f/50 testing, respectively. In Figure A-4 the LUPI diverger lens ("f.l. = 7.0 cm") is shown inside the chamber, rather than in its usual position, fastened to the LUPI. This repositioning was required so that the vacuum chamber window would be in the collimated beam between the beam divider and the diverger. If the window had been in the converging f/3.85 beam between the primary and the diverger it would have produced a large amount of spherical aberration, making alignment and data reduction more difficult.

Details of the Newtonian flat used in Figure A-4 are shown in Figure A-6.

The test flat, which was supplied by MSFC, was mounted in an aluminum ring by Tinsley Laboratories, using RTV (room-temperature vulcanizing) silicone rubber. This ring was in turn mounted to an auxiliary plate, which was in turn mounted to the end plate of the vacuum chamber. The tilt of the auxiliary plate relative to the end plate was adjustable through vacuum feedthroughs from outside the chamber. This saved time by permitting adjustment of the flat relative to the FVU without bleeding up the chamber.

Output maps of wavefronts from the MSFC test flat are shown in Figures A-7 and A-8 in units of 0.01 (λ = 6328 Å). These maps are of wavefronts produced at 45° angle of incidence, and the flat was double-passed during these tests.

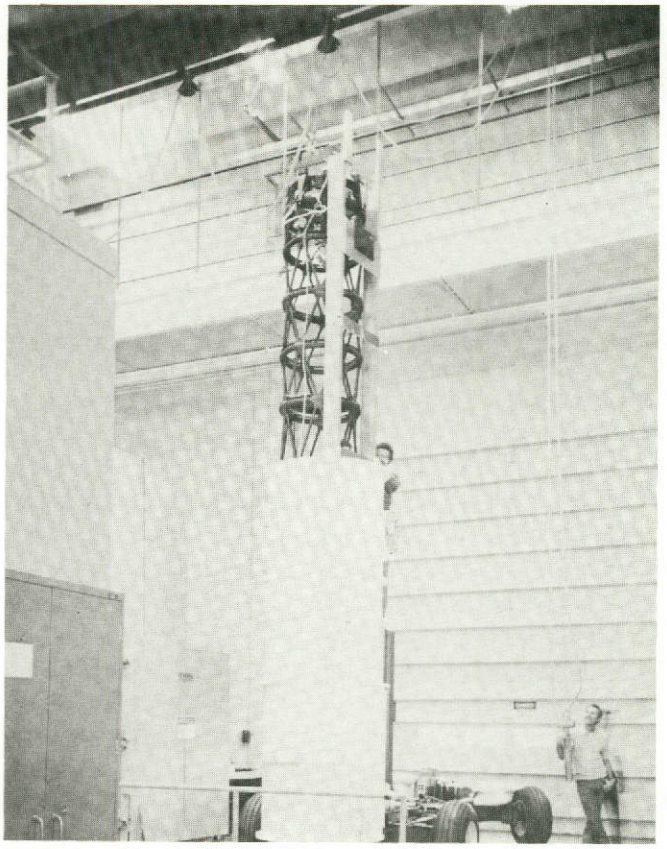

Figure A-3 PHG Chamber Vertical

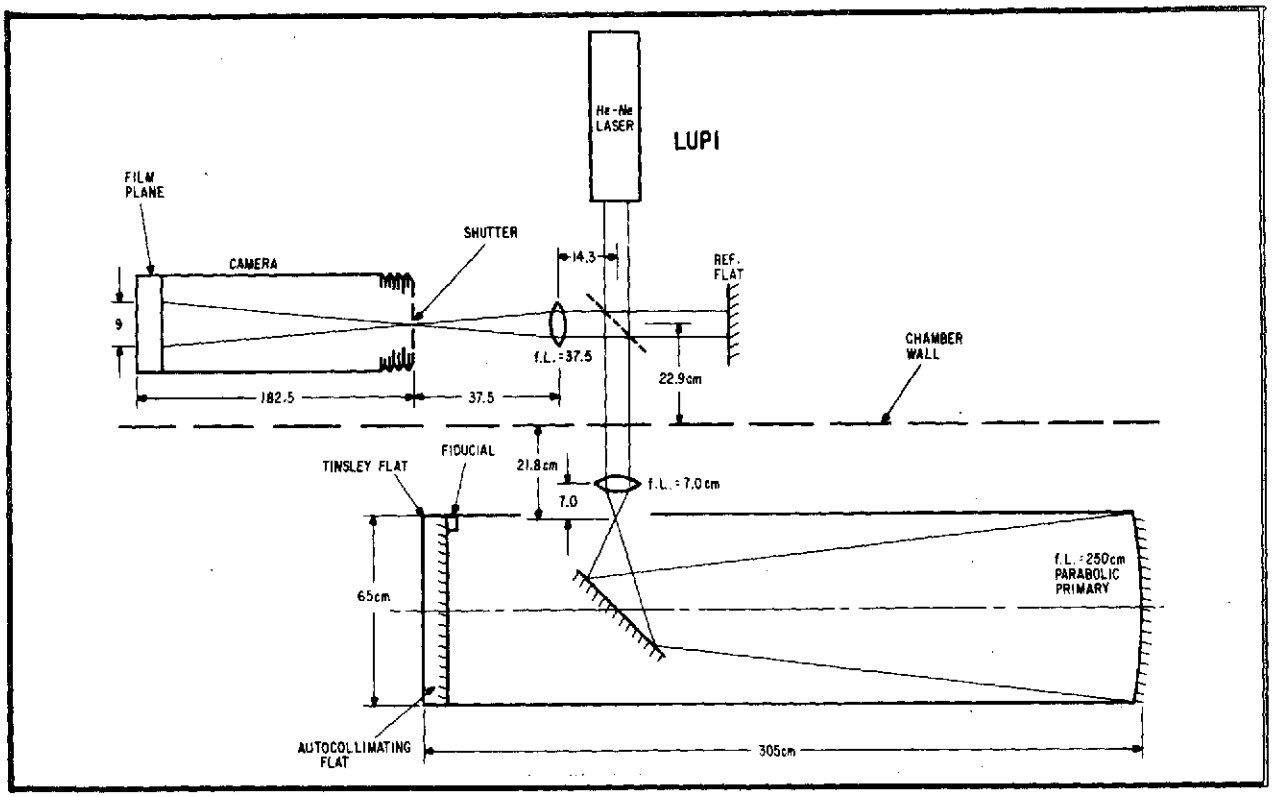

Figure A-4 Optical Test for Primary Mirror Gravity Effects

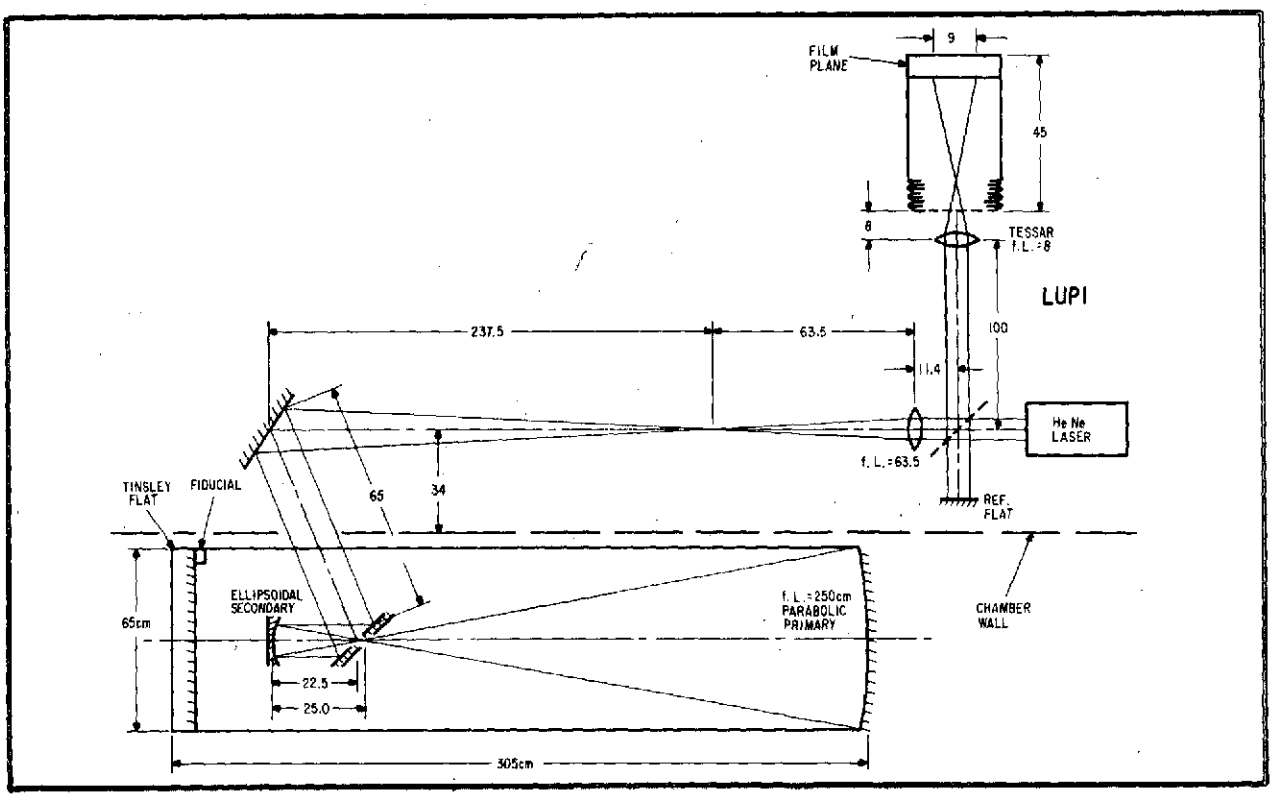

Figure A-5 Optical Test of Assembled System

F73-04

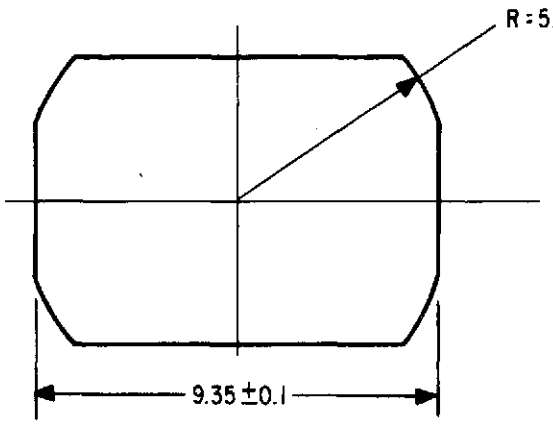

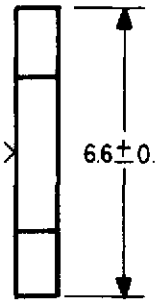

NOTES

1. ALL DIMENSIONS ARE IN INCHES
2. FLAT SIDE ALUMINIZED WITH A SILICON MONOXIDE PROTECTIVE COATING
3. ALUMINIZE FLAT SIDE WITH A SILICON MONOXIDE PROTECTIVE COATING
4. BREAK ALL EDGES

GLASS	THICKNESS	FLAT SURFACE	BACK SURFACE
10-INCH CERVIT OR ULE EQUIVA-LENT	1.7 $^{+0.00}_{-0.25}$ PARALLELISM IS $\pm$ .010	FLATNESS: $\frac{\lambda}{8}$ (λ = 589.3 nm) QUALITY: 80-50 OR BETTER	FINE GRIND

Figure A-6 Newtonian Flat

1	0	0	0	0	0	0	0	0	0	0	0	3	12	12	10	5	1	-1	0	0	0	0	0	0	0	0	0	0	0	0	0
2	0	0	0	0	0	0	0	0	0	5	3	5	9	9	7	3	1	0	0	0	0	0	0	0	0	0	0	0	0	0	0
3	0	0	0	0	14	10	8	10	10	9	7	6	6	5	4	1	1	2	0	-2	-7	0	0	0	0	0	0	0	0	0	0
4	0	0	0	0	13	10	10	11	9	6	5	3	0	0	0	-3	-4	-4	-2	-2	-5	0	0	0	0	0	0	0	0	0	0
5	0	0	0	0	12	11	11	12	8	4	3	0	-5	-4	-5	-9	-11	-10	-5	-2	-3	-7	-13	-25	-38	0	0	0	0	0	0
6	0	0	0	0	9	8	10	12	6	1	0	-3	-6	-8	-8	-9	-9	-8	-5	-3	-4	-6	-10	-17	-25	0	0	0	0	0	0
7	0	0	0	7	5	5	8	12	4	-2	-3	-7	-12	-13	-12	-8	-7	-5	-5	-5	-4	-6	-7	-8	-12	-18	0	0	0	0	0
8	0	0	0	7	6	6	6	5	0	-3	-6	-8	-10	-11	-11	-8	-7	-7	-5	-4	-5	-4	-4	-5	-9	-15	0	0	0	0	0
9	0	0	0	7	7	6	3	-1	-2	-5	-9	-10	-8	-10	-11	-8	-8	-8	-5	-4	-5	-3	-2	-1	-5	-11	-20	0	0	0	0
10	0	0	0	7	7	9	5	0	-1	-3	-5	-7	-8	-9	-9	-6	-6	-6	-4	-4	-5	-4	-4	-3	-4	-6	-14	0	0	0	0
11	0	0	8	7	8	11	7	2	0	0	0	-4	-8	-8	-6	-4	-5	-5	-3	-4	-5	-6	-5	-4	-2	-2	-8	0	0	0	0
12	0	0	8	7	8	10	6	1	-1	-2	-1	-3	-4	-3	-3	-4	-4	-3	-2	-2	-3	-3	-3	-3	-1	0	-4	0	0	0	0
13	0	0	7	8	8	9	5	0	-3	-4	-2	-1	-1	0	-1	-4	-3	-2	-1	0	0	-1	-2	-2	0	2	0	-4	-9	0	0
14	0	0	7	6	6	7	3	0	-2	-3	-1	0	1	2	0	-2	0	0	0	1	2	2	2	1	3	4	0	-2	0	0	0
15	0	0	7	5	4	5	2	-1	-1	-1	-1	3	5	3	1	-1	2	3	1	3	5	7	6	5	7	6	2	0	0	0	0
16	0	0	3	3	4	5	1	0	-2	-1	0	2	4	5	1	0	2	2	0	3	5	6	5	5	7	7	5	2	0	0	0
17	0	0	0	2	3	4	1	0	-2	0	2	2	3	6	2	0	1	0	-1	3	6	5	5	5	7	8	7	4	0	0	0
18	0	0	0	0	1	1	1	0	-1	0	1	1	0	1	1	1	4	3	1	4	6	7	5	4	8	9	8	4	0	0	0
19	0	0	-1	-1	-1	0	0	1	0	0	1	0	-1	-2	0	2	6	6	4	5	7	10	6	4	9	10	9	3	0	0	0
20	0	0	-1	-4	-3	0	0	-1	-3	-2	-1	-1	-1	-1	-1	0	6	5	4	5	7	9	6	6	10	9	6	3	0	0	0
21	0	0	-2	-7	-6	0	-2	-4	-7	-6	-3	-2	-1	0	-2	-1	5	5	4	5	6	8	7	7	11	8	3	3	0	0	0
22	0	0	-4	-8	-7	-2	-2	-3	-4	-4	-3	-2	-2	-2	-2	0	3	5	6	5	5	8	9	10	12	9	5	4	0	0	0
23	0	0	-6	-9	-8	-4	-1	-1	-1	-2	-2	-2	-2	-3	-1	0	2	6	8	4	4	7	11	12	12	10	7	4	0	0	0
24	0	0	0	0	-8	-4	-3	-2	-1	-1	-1	-2	-2	-3	-1	0	3	6	7	6	6	7	9	11	12	9	0	0	0	0	0
25	0	0	0	0	-9	-5	-4	-3	-1	-1	-1	-2	-3	-3	-1	1	5	6	7	7	7	7	8	10	12	9	0	0	0	0	0
26	0	0	0	0	0	-8	-6	-4	-2	-1	0	-2	-2	-1	-1	0	4	5	6	8	8	8	11	12	0	0	0	0	0	0	0
27	0	0	0	0	0	-12	-7	-5	-3	-1	0	-2	-1	0	-1	0	2	4	6	9	8	9	15	14	0	0	0	0	0	0	0
28	0	0	0	0	0	-11	-9	-8	-7	-5	-3	-4	-2	-1	-1	0	2	4	6	9	8	7	7	0	0	0	0	0	0	0	0
29	0	0	0	0	0	-11	-11	-11	-12	-8	-6	-6	-3	-2	-1	0	2	4	6	9	7	5	0	0	0	0	0	0	0	0	0
30	0	0	0	0	0	0	0	-13	-15	-11	-8	-8	-4	-2	-4	-3	-2	0	1	2	0	0	0	0	0	0	0	0	0	0	0
31	0	0	0	0	0	0	0	-14	-17	-13	-10	-10	-6	-3	-6	-7	-7	-5	-4	-4	0	0	0	0	0	0	0	0	0	0	0

Figure A-7 Wavefront Map of MSFC Test Flat, No. 914 Focus Run (Table 3-2)

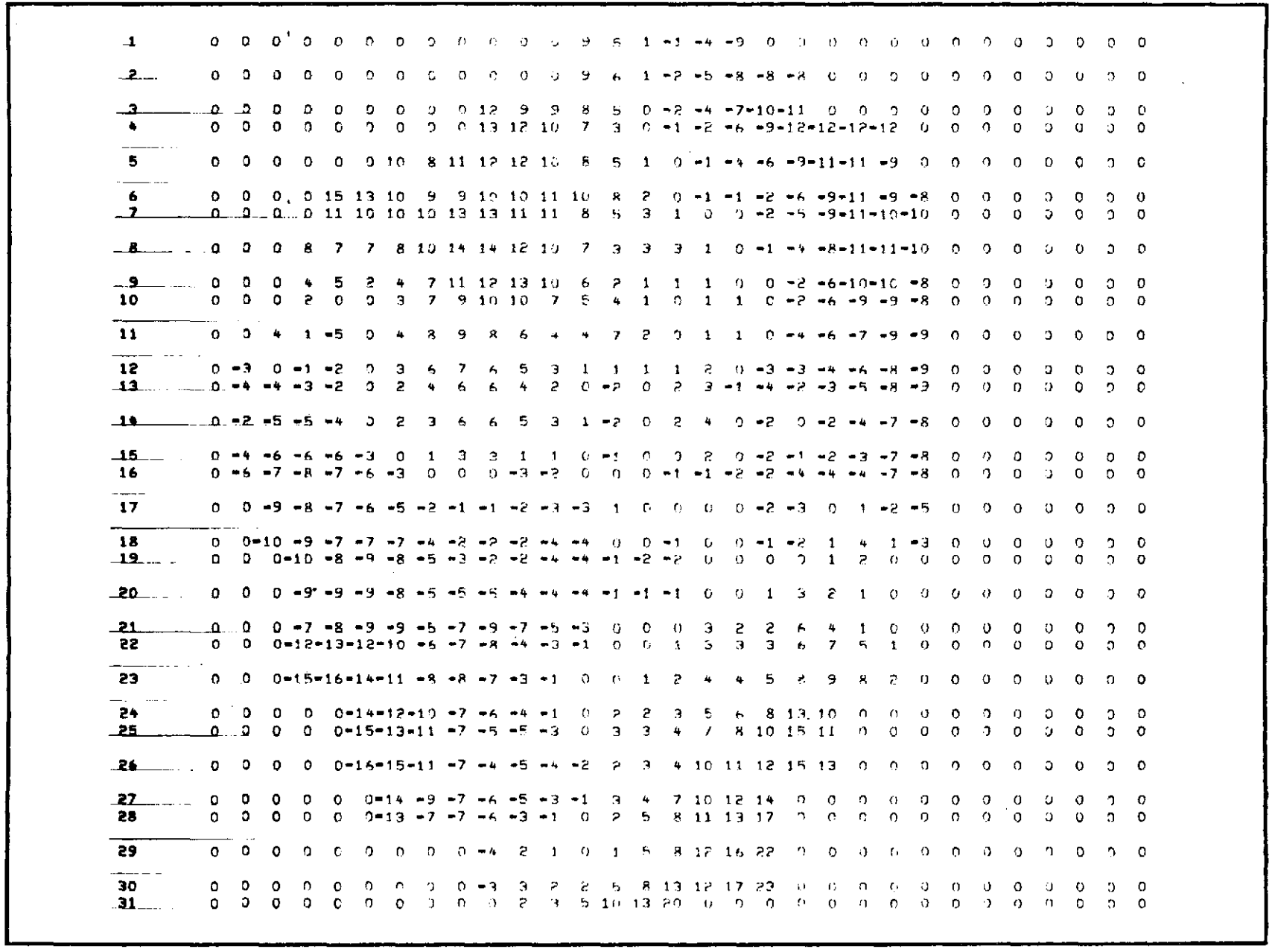

1	0	0	0	0	0	0	0	0	0	0	0	0	9	5	1	-1	-4	-9	0	0	0	0	0	0	0	0	0	0	0	0
2	0	0	0	0	0	0	0	0	0	0	0	0	9	6	1	-2	-5	-8	-8	-8	0	0	0	0	0	0	0	0	0	0
3	0	0	0	0	0	0	0	0	0	12	9	9	8	5	0	-2	-4	-7	-10	-11	0	0	0	0	0	0	0	0	0	0
4	0	0	0	0	0	0	0	0	0	13	12	10	7	3	0	-1	-2	-6	-9	-12	-12	-12	-12	0	0	0	0	0	0	0
5	0	0	0	0	0	0	10	8	11	12	12	10	6	5	1	0	-1	-4	-6	-9	-11	-11	-9	0	0	0	0	0	0	0
6	0	0	0	0	15	13	10	9	9	10	10	11	10	8	2	0	-1	-1	-2	-6	-9	-11	-9	-8	0	0	0	0	0	0
7	0	0	0	0	11	10	10	10	13	13	11	11	8	5	3	1	0	0	-2	-5	-9	-11	-10	-10	0	0	0	0	0	0
8	0	0	0	8	7	7	8	10	14	14	12	10	7	3	3	3	1	0	-1	-4	-8	-11	-11	-10	0	0	0	0	0	0
9	0	0	0	4	5	2	4	7	11	12	13	10	6	2	1	1	1	0	0	-2	-6	-10	-10	-8	0	0	0	0	0	0
10	0	0	0	2	0	0	3	7	9	10	10	7	5	4	1	0	1	1	0	-2	-6	-9	-9	-8	0	0	0	0	0	0
11	0	0	4	1	-5	0	4	8	9	8	6	4	4	7	2	0	1	1	0	-4	-6	-7	-9	-9	0	0	0	0	0	0
12	0	-3	0	-1	-2	0	3	6	7	6	5	3	1	1	1	1	2	0	-3	-3	-4	-6	-8	-9	0	0	0	0	0	0
13	0	-4	-4	-3	-2	0	2	4	6	6	4	2	0	-2	0	2	3	-1	-4	-2	-3	-5	-8	-9	0	0	0	0	0	0
14	0	-2	-5	-5	-4	0	2	3	6	6	5	3	1	-2	0	2	4	0	-2	0	-2	-4	-7	-8	0	0	0	0	0	0
15	0	-4	-6	-6	-6	-3	0	1	3	3	1	1	0	-1	0	0	2	0	-2	-1	-2	-3	-7	-8	0	0	0	0	0	0
16	0	-6	-7	-8	-7	-6	-3	0	0	0	-3	-2	0	0	0	-1	-1	-2	-2	-4	-4	-4	-7	-8	0	0	0	0	0	0
17	0	0	-9	-8	-7	-6	-5	-2	-1	-1	-2	-3	-3	1	0	0	0	0	-2	-3	0	1	-2	-5	0	0	0	0	0	0
18	0	0	-10	-9	-7	-7	-7	-4	-2	-2	-2	-4	-4	0	0	-1	0	0	-1	-2	1	4	1	-3	0	0	0	0	0	0
19	0	0	0	-10	-8	-9	-8	-5	-3	-2	-2	-4	-4	-1	-2	-2	0	0	0	0	1	2	0	0	0	0	0	0	0	0
20	0	0	0	-9	-9	-9	-8	-5	-5	-5	-4	-4	-4	-1	-1	-1	0	0	1	3	2	1	0	0	0	0	0	0	0	0
21	0	0	0	-7	-8	-9	-9	-6	-7	-9	-7	-6	-3	0	0	0	3	2	2	6	4	1	0	0	0	0	0	0	0	0
22	0	0	0	-12	-13	-12	-10	-6	-7	-8	-4	-3	-1	0	0	1	5	3	3	6	7	5	1	0	0	0	0	0	0	0
23	0	0	0	-15	-16	-14	-11	-8	-8	-7	-3	-1	0	0	1	2	4	4	5	8	9	8	2	0	0	0	0	0	0	0
24	0	0	0	0	0	-14	-12	-10	-7	-6	-4	-1	0	2	2	3	5	6	8	13	10	0	0	0	0	0	0	0	0	0
25	0	0	0	0	0	-15	-13	-11	-7	-5	-5	-3	0	3	3	4	7	8	10	15	11	0	0	0	0	0	0	0	0	0
26	0	0	0	0	0	-16	-15	-11	-7	-4	-5	-4	-2	2	3	4	10	11	12	15	13	0	0	0	0	0	0	0	0	0
27	0	0	0	0	0	0	-14	-9	-7	-6	-5	-3	-1	3	4	7	10	12	14	0	0	0	0	0	0	0	0	0	0	0
28	0	0	0	0	0	0	-13	-7	-7	-6	-3	-1	0	2	5	8	11	13	17	0	0	0	0	0	0	0	0	0	0	0
29	0	0	0	0	0	0	0	0	0	-4	2	1	0	1	5	8	12	16	22	0	0	0	0	0	0	0	0	0	0	0
30	0	0	0	0	0	0	0	0	0	-3	3	2	2	5	8	13	12	17	23	0	0	0	0	0	0	0	0	0	0	0
31	0	0	0	0	0	0	0	0	0	0	2	3	5	10	13	20	0	0	0	0	0	0	0	0	0	0	0	0	0	0

Figure A-8 Wavefront Map of MSFC Test Flat, No. 923 Focus Run (Table 3-2)

Appendix B
DATA REDUCTION

Data reduction starts with the Type 57 Polaroid positive interferogram. The operator digitizes the interferogram in X-Y coordinates for approximately 300 points on a typical picture, the points giving the locations of interference fringes on the print. One fringe is selected as a reference fringe, the points of which are identified to permit the computer later to sort out the order number of each fringe. The location of fiducial marks around the border of the test aperture are also digitized.

The data are then put through the surface-fitting routines, which fit the test wavefront (which is implicit in the fringe pattern of the interferogram) to various reference wavefronts, such as a plane, a sphere, or a cylinder. The particular surface chosen represents an image aberration; for example, a sphere in characteristic of defocus, and a cylinder of astigmatism. (A plane, the limiting case, represents a perfect wavefront.) The amount of each aberration for an interferogram is determined by the best fitting reference surfaces. The program finds the best fitting (in the root-mean-square sense) reference surface as specified, then prints out a 31 x 31 matrix of the differences between the reference surface and the test wavefront, as well as the rms, average, and peak values of this matrix.

Also available are routines for averaging several experimental wavefronts, and for subtracting one wavefront from another. The latter routine was to be used in precise analysis of the effects of gravity orientation and to subtract out the imperfection of the reference flat. This was not done since the large wavefront errors encountered made alignment difficult, introduced sampling errors into the surface-fitting process, and were much larger than the errors of the reference flat.

Alignment was difficult because the usual indication of a good wavefront - straight, evenly-spaced fringes - was never present. Sampling errors were introduced by the irregular spacing of the fringes; there were simply more data points in regions where fringes were more closely spaced, and the program makes no provision for non-uniform data density. For this reason, interferograms otherwise identical, but with different fringe orientations, give different "best-fit" reference surfaces as well as different residual errors.

Figures B-1 through B-6 show a typical interferogram and the matrices resulting after fitting an interferogram to various computer routines. Matrix values are in units of $\lambda/100$.

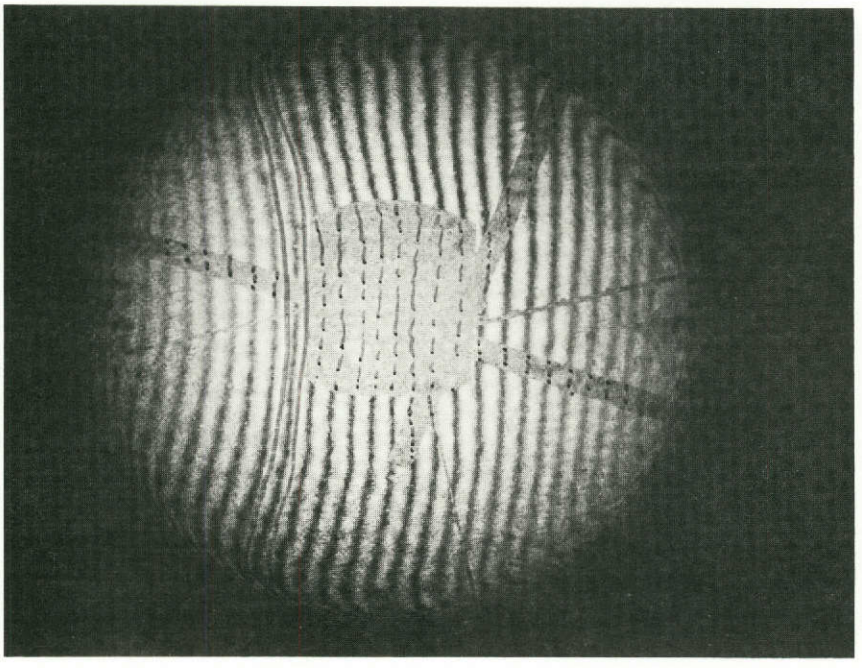

Figure B-1 Typical Interferogram

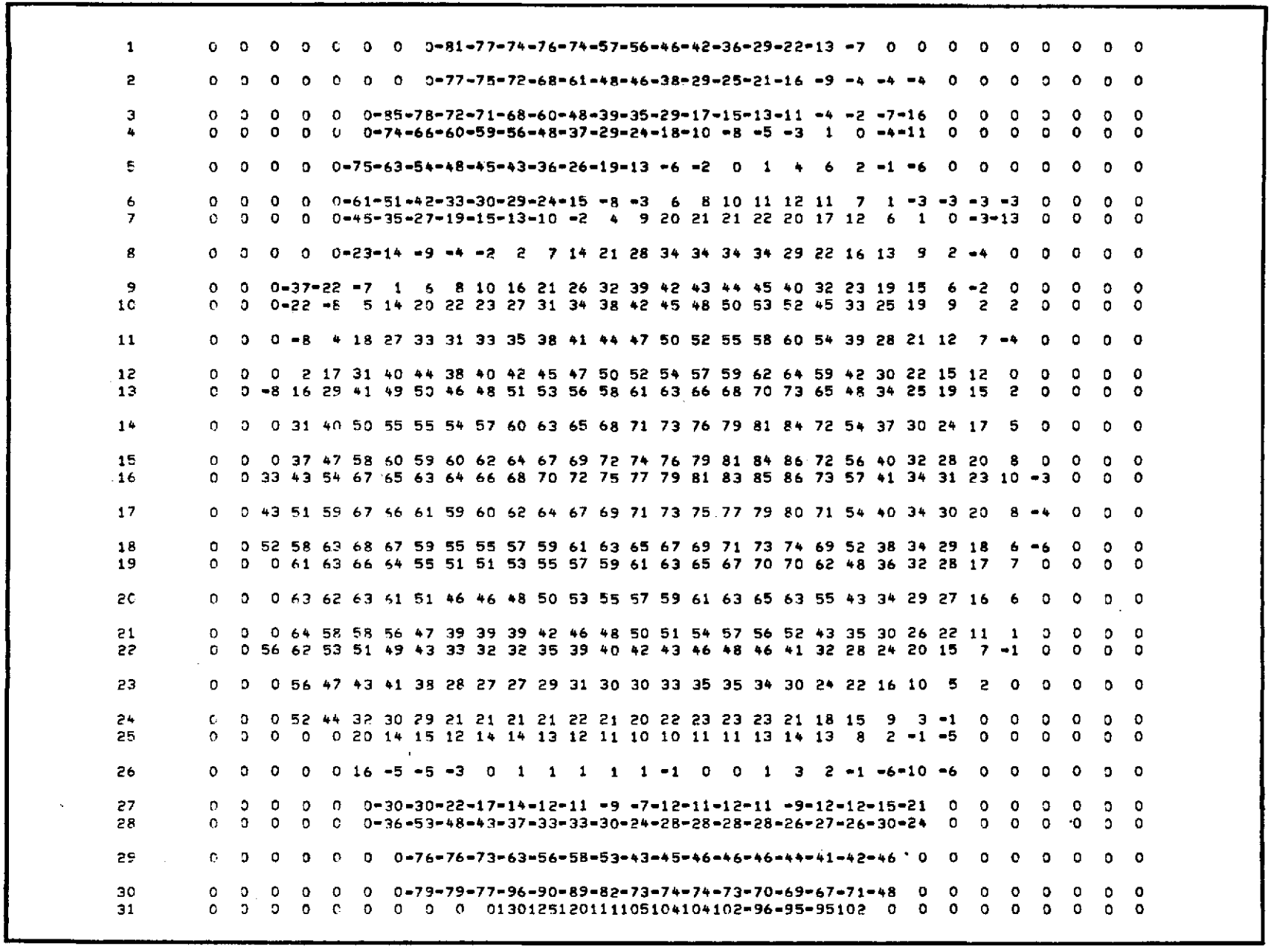

```
 1      0  0  0  0  0  0  0  0-81-77-74-76-74-57-56-46-42-36-29-22-13 -7  0  0  0  0  0  0  0  0  0
 2      0  0  0  0  0  0  0  0-77-75-72-68-61-48-46-38-29-25-21-16 -9 -4 -4 -4  0  0  0  0  0  0  0
 3      0  0  0  0  0  0-85-78-72-71-68-60-48-39-35-29-17-15-13-11 -4 -2 -7-16  0  0  0  0  0  0  0
 4      0  0  0  0  0  0-74-66-60-59-56-48-37-29-24-18-10 -8 -5 -3  1  0 -4-11  0  0  0  0  0  0  0
 5      0  0  0  0  0-75-63-54-48-45-43-36-26-19-13 -6 -2  0  1  4  6  2 -1 -6  0  0  0  0  0  0  0
 6      0  0  0  0  0-61-51-42-33-30-29-24-15 -8 -3  6  8 10 11 12 11  7  1 -3 -3 -3 -3  0  0  0  0
 7      0  0  0  0  0-45-35-27-19-15-13-10 -2  4  9 20 21 21 22 20 17 12  6  1  0 -3-13  0  0  0  0
 8      0  0  0  0  0-23-14 -9 -4 -2  2  7 14 21 28 34 34 34 34 29 22 16 13  9  2 -4  0  0  0  0  0
 9      0  0  0-37-22 -7  1  6  8 10 16 21 26 32 39 42 43 44 45 40 32 23 19 15  6 -2  0  0  0  0  0
10      0  0  0-22 -8  5 14 20 22 23 27 31 34 38 42 45 48 50 53 52 45 33 25 19  9  2  2  0  0  0  0
11      0  0  0 -8  4 18 27 33 31 33 35 38 41 44 47 50 52 55 58 60 54 39 28 21 12  7 -4  0  0  0  0
12      0  0  0  2 17 31 40 44 38 40 42 45 47 50 52 54 57 59 62 64 59 42 30 22 15 12  0  0  0  0  0
13      0  0 -8 16 29 41 49 50 46 48 51 53 56 58 61 63 66 68 70 73 65 48 34 25 19 15  2  0  0  0  0
14      0  0  0 31 40 50 55 55 54 57 60 63 65 68 71 73 76 79 81 84 72 54 37 30 24 17  5  0  0  0  0
15      0  0  0 37 47 58 60 59 60 62 64 67 69 72 74 76 79 81 84 86 72 56 40 32 28 20  8  0  0  0  0
16      0  0 33 43 54 67 65 63 64 66 68 70 72 75 77 79 81 83 85 86 73 57 41 34 31 23 10 -3  0  0  0
17      0  0 43 51 59 67 66 61 59 60 62 64 67 69 71 73 75 77 79 80 71 54 40 34 30 20  8 -4  0  0  0
18      0  0 52 58 63 68 67 59 55 55 57 59 61 63 65 67 69 71 73 74 69 52 38 34 29 18  6 -6  0  0  0
19      0  0  0 61 63 66 64 55 51 51 53 55 57 59 61 63 65 67 70 70 62 48 36 32 28 17  7  0  0  0  0
20      0  0  0 63 62 63 61 51 46 46 48 50 53 55 57 59 61 63 65 63 55 43 34 29 27 16  6  0  0  0  0
21      0  0  0 64 58 58 56 47 39 39 39 42 46 48 50 51 54 57 56 52 43 35 30 26 22 11  1  0  0  0  0
22      0  0 56 62 53 51 49 43 33 32 32 35 39 40 42 43 46 48 46 41 32 28 24 20 15  7 -1  0  0  0  0
23      0  0  0 56 47 43 41 38 28 27 27 29 31 30 30 33 35 35 34 30 24 22 16 10  5  2  0  0  0  0  0
24      0  0  0 52 44 32 30 29 21 21 21 21 22 21 20 22 23 23 23 21 18 15  9  3 -1  0  0  0  0  0  0
25      0  0  0  0  0 20 14 15 12 14 14 13 12 11 10 10 11 11 13 14 13  8  2 -1 -5  0  0  0  0  0  0
26      0  0  0  0  0 16 -5 -5 -3  0  1  1  1  1  1 -1  0  0  1  3  2 -1 -6-10 -6  0  0  0  0  0  0
27      0  0  0  0  0  0-30-30-22-17-14-12-11 -9 -7-12-11-12-11 -9-12-12-15-21  0  0  0  0  0  0  0
28      0  0  0  0  0  0-36-53-48-43-37-33-33-30-24-28-28-28-28-26-27-26-30-24  0  0  0  0  0  0  0
29      0  0  0  0  0  0  0-76-76-73-63-56-58-53-43-45-46-46-46-44-41-42-46  0  0  0  0  0  0  0  0
30      0  0  0  0  0  0  0-79-79-77-96-90-89-82-73-74-74-73-70-69-67-71-48  0  0  0  0  0  0  0  0
31      0  0  0  0  0  0  0  0  0 0130125120111105104104102-96-95-95102  0  0  0  0  0  0  0  0  0
```

Figure B-2 "No-Focus" Output Map

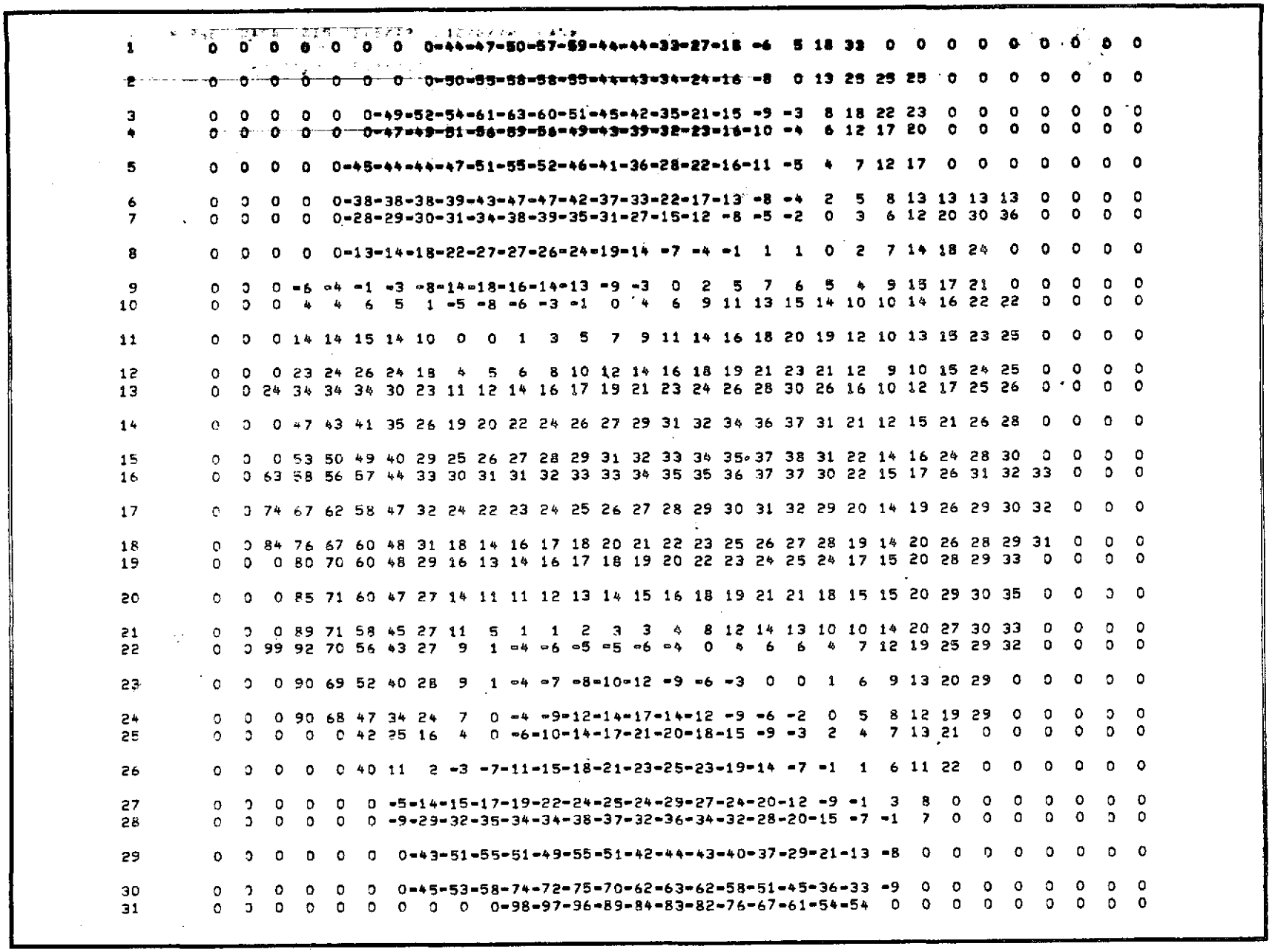

1	0	0	0	0	0	0	0	0	-44	-47	-50	-57	-59	-44	-44	-33	-27	-18	-6	5	18	33	0	0	0	0	0	0	0	0	0
2	0	0	0	0	0	0	0	0	-50	-55	-58	-58	-55	-44	-43	-34	-24	-16	-8	0	13	25	25	25	0	0	0	0	0	0	0
3	0	0	0	0	0	0	-49	-52	-54	-61	-63	-60	-51	-45	-42	-35	-21	-15	-9	-3	8	18	22	23	0	0	0	0	0	0	0
4	0	0	0	0	0	0	-47	-49	-51	-56	-59	-56	-49	-43	-39	-32	-23	-16	-10	-4	6	12	17	20	0	0	0	0	0	0	0
5	0	0	0	0	0	-45	-44	-44	-47	-51	-55	-52	-46	-41	-36	-28	-22	-16	-11	-5	4	7	12	17	0	0	0	0	0	0	0
6	0	0	0	0	0	-38	-38	-38	-39	-43	-47	-47	-42	-37	-33	-22	-17	-13	-8	-4	2	5	8	13	13	13	13	0	0	0	0
7	0	0	0	0	0	-28	-29	-30	-31	-34	-38	-39	-35	-31	-27	-15	-12	-8	-5	-2	0	3	6	12	20	30	36	0	0	0	0
8	0	0	0	0	0	-13	-14	-18	-22	-27	-27	-26	-24	-19	-14	-7	-4	-1	1	1	0	2	7	14	18	24	0	0	0	0	0
9	0	0	0	-6	-4	-1	-3	-8	-14	-18	-16	-14	-13	-9	-3	0	2	5	7	6	5	4	9	15	17	21	0	0	0	0	0
10	0	0	0	4	4	6	5	1	-5	-8	-6	-3	-1	0	4	6	9	11	13	15	14	10	10	14	16	22	22	0	0	0	0
11	0	0	0	14	14	15	14	10	0	0	1	3	5	7	9	11	14	16	18	20	19	12	10	13	15	23	25	0	0	0	0
12	0	0	0	23	24	26	24	18	4	5	6	8	10	12	14	16	18	19	21	23	21	12	9	10	15	24	25	0	0	0	0
13	0	0	24	34	34	34	30	23	11	12	14	16	17	19	21	23	24	26	28	30	26	16	10	12	17	25	26	0	0	0	0
14	0	0	0	47	43	41	35	26	19	20	22	24	26	27	29	31	32	34	36	37	31	21	12	15	21	26	28	0	0	0	0
15	0	0	0	53	50	49	40	29	25	26	27	28	29	31	32	33	34	35	37	38	31	22	14	16	24	28	30	0	0	0	0
16	0	0	63	58	56	57	44	33	30	31	31	32	33	33	34	35	35	36	37	37	30	22	15	17	26	31	32	33	0	0	0
17	0	0	74	67	62	58	47	32	24	22	23	24	25	26	27	28	29	30	31	32	29	20	14	19	26	29	30	32	0	0	0
18	0	0	84	76	67	60	48	31	18	14	16	17	18	20	21	22	23	25	26	27	28	19	14	20	26	28	29	31	0	0	0
19	0	0	0	80	70	60	48	29	16	13	14	16	17	18	19	20	22	23	24	25	24	17	15	20	28	29	33	0	0	0	0
20	0	0	0	85	71	60	47	27	14	11	11	12	13	14	15	16	18	19	21	21	18	15	15	20	29	30	35	0	0	0	0
21	0	0	0	89	71	58	45	27	11	5	1	1	2	3	3	4	8	12	14	13	10	10	14	20	27	30	33	0	0	0	0
22	0	0	99	92	70	56	43	27	9	1	-4	-6	-5	-5	-6	-4	0	4	6	6	4	7	12	19	25	29	32	0	0	0	0
23	0	0	0	90	69	52	40	28	9	1	-4	-7	-8	-10	-12	-9	-6	-3	0	0	1	6	9	13	20	29	0	0	0	0	0
24	0	0	0	90	68	47	34	24	7	0	-4	-9	-12	-14	-17	-14	-12	-9	-6	-2	0	5	8	12	19	29	0	0	0	0	0
25	0	0	0	0	0	42	25	16	4	0	-6	-10	-14	-17	-21	-20	-18	-15	-9	-3	2	4	7	13	21	0	0	0	0	0	0
26	0	0	0	0	0	40	11	2	-3	-7	-11	-15	-18	-21	-23	-25	-23	-19	-14	-7	-1	1	6	11	22	0	0	0	0	0	0
27	0	0	0	0	0	0	-5	-14	-15	-17	-19	-22	-24	-25	-24	-29	-27	-24	-20	-12	-9	-1	3	8	0	0	0	0	0	0	0
28	0	0	0	0	0	0	-9	-29	-32	-35	-34	-34	-38	-37	-32	-36	-34	-32	-28	-20	-15	-7	-1	7	0	0	0	0	0	0	0
29	0	0	0	0	0	0	0	-43	-51	-55	-51	-49	-55	-51	-42	-44	-43	-40	-37	-29	-21	-13	-8	0	0	0	0	0	0	0	0
30	0	0	0	0	0	0	0	-45	-53	-58	-74	-72	-75	-70	-62	-63	-62	-58	-51	-45	-36	-33	-9	0	0	0	0	0	0	0	0
31	0	0	0	0	0	0	0	0	0	0	-98	-97	-96	-89	-84	-83	-82	-76	-67	-61	-54	-54	0	0	0	0	0	0	0	0	0

Figure B-3 "Focus" Output Map

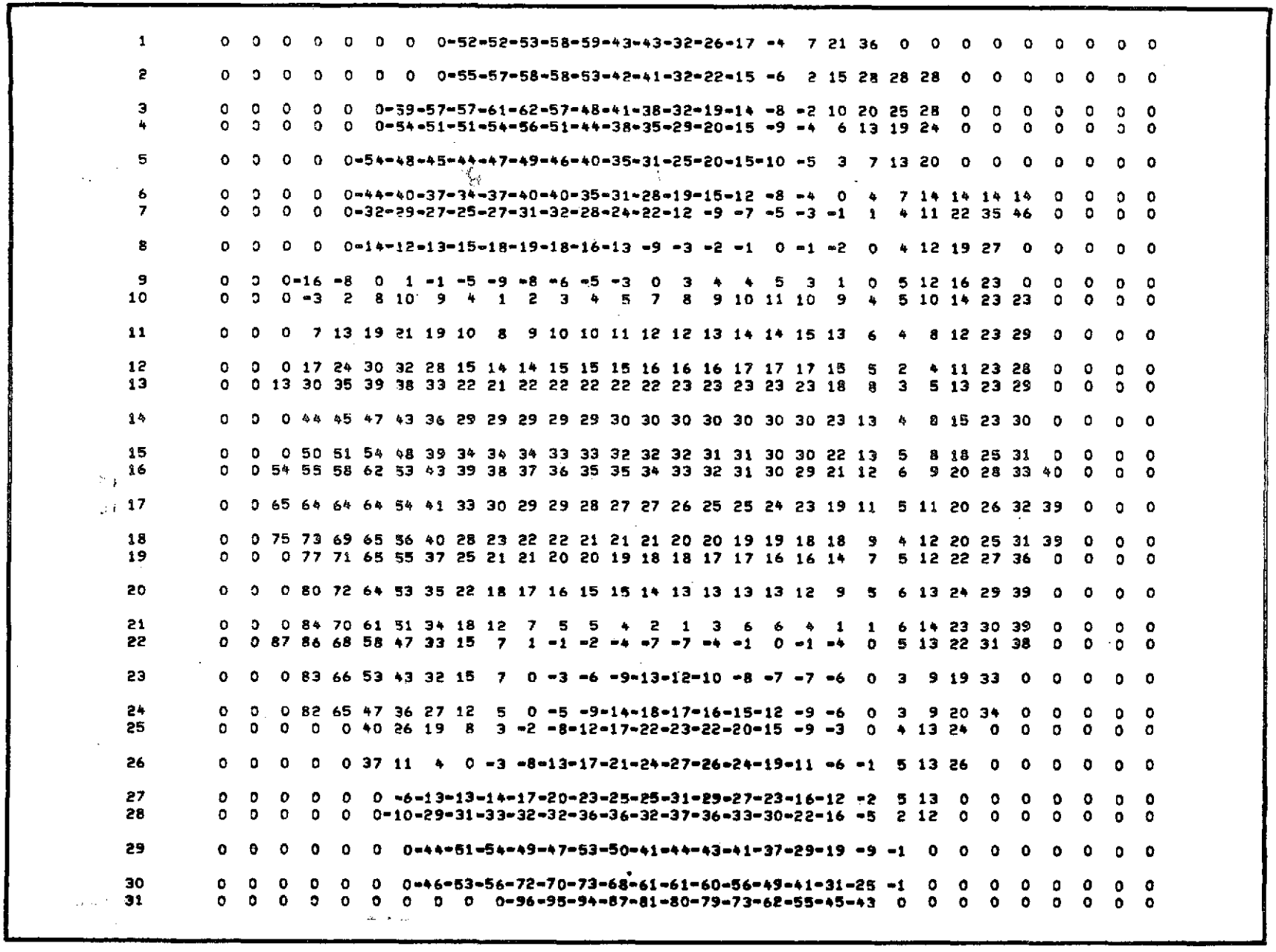

```
 1      0  0  0  0  0  0  0  0-52-52-53-58-59-43-43-32-26-17 -4  7 21 36  0  0  0  0  0  0  0  0  0
 2      0  0  0  0  0  0  0  0-55-57-58-58-53-42-41-32-22-15 -6  2 15 28 28 28  0  0  0  0  0  0  0
 3      0  0  0  0  0  0-59-57-57-61-62-57-48-41-38-32-19-14 -8 -2 10 20 25 28  0  0  0  0  0  0  0
 4      0  0  0  0  0  0-54-51-51-54-56-51-44-38-35-29-20-15 -9 -4  6 13 19 24  0  0  0  0  0  0  0
 5      0  0  0  0  0-54-48-45-44-47-49-46-40-35-31-25-20-15-10 -5  3  7 13 20  0  0  0  0  0  0  0
 6      0  0  0  0  0-44-40-37-34-37-40-40-35-31-28-19-15-12 -8 -4  0  4  7 14 14 14 14  0  0  0  0
 7      0  0  0  0  0-32-29-27-25-27-31-32-28-24-22-12 -9 -7 -5 -3 -1  1  4 11 22 35 46  0  0  0  0
 8      0  0  0  0  0-14-12-13-15-18-19-18-16-13 -9 -3 -2 -1  0 -1 -2  0  4 12 19 27  0  0  0  0  0
 9      0  0  0-16 -8  0  1 -1 -5 -9 -8 -6 -5 -3  0  3  4  4  5  3  1  0  5 12 16 23  0  0  0  0  0
10      0  0  0 -3  2  8 10  9  4  1  2  3  4  5  7  8  9 10 11 10  9  4  5 10 14 23 23  0  0  0  0
11      0  0  0  7 13 19 21 19 10  8  9 10 10 11 12 12 13 14 14 15 13  6  4  8 12 23 29  0  0  0  0
12      0  0  0 17 24 30 32 28 15 14 14 15 15 15 16 16 16 17 17 17 15  5  2  4 11 23 28  0  0  0  0
13      0  0 13 30 35 39 38 33 22 21 22 22 22 22 22 23 23 23 23 23 18  8  3  5 13 23 29  0  0  0  0
14      0  0  0 44 45 47 43 36 29 29 29 29 29 30 30 30 30 30 30 30 23 13  4  8 15 23 30  0  0  0  0
15      0  0  0 50 51 54 48 39 34 34 34 33 33 32 32 32 31 31 30 30 22 13  5  8 18 25 31  0  0  0  0
16      0  0 54 55 58 62 53 43 39 38 37 36 35 35 34 33 32 31 30 29 21 12  6  9 20 28 33 40  0  0  0
17      0  0 65 64 64 64 54 41 33 30 29 29 28 27 27 26 25 25 24 23 19 11  5 11 20 26 32 39  0  0  0
18      0  0 75 73 69 65 56 40 28 23 22 22 21 21 21 20 20 19 19 18 18  9  4 12 20 25 31 39  0  0  0
19      0  0  0 77 71 65 55 37 25 21 21 20 20 19 18 18 17 17 16 16 14  7  5 12 22 27 36  0  0  0  0
20      0  0  0 80 72 64 53 35 22 18 17 16 15 15 14 13 13 13 13 12  9  5  6 13 24 29 39  0  0  0  0
21      0  0  0 84 70 61 51 34 18 12  7  5  5  4  2  1  3  6  6  4  1  1  6 14 23 30 39  0  0  0  0
22      0  0 87 86 68 58 47 33 15  7  1 -1 -2 -4 -7 -7 -4 -1  0 -1 -4  0  5 13 22 31 38  0  0  0  0
23      0  0  0 83 66 53 43 32 15  7  0 -3 -6 -9-13-12-10 -8 -7 -7 -6  0  3  9 19 33  0  0  0  0  0
24      0  0  0 82 65 47 36 27 12  5  0 -5 -9-14-18-17-16-15-12 -9 -6  0  3  9 20 34  0  0  0  0  0
25      0  0  0  0  0 40 26 19  8  3 -2 -8-12-17-22-23-22-20-15 -9 -3  0  4 13 24  0  0  0  0  0  0
26      0  0  0  0  0 37 11  4  0 -3 -8-13-17-21-24-27-26-24-19-11 -6 -1  5 13 26  0  0  0  0  0  0
27      0  0  0  0  0  0 -6-13-13-14-17-20-23-25-25-31-29-27-23-16-12 -2  5 13  0  0  0  0  0  0  0
28      0  0  0  0  0  0-10-29-31-33-32-32-36-36-32-37-36-33-30-22-16 -5  2 12  0  0  0  0  0  0  0
29      0  0  0  0  0  0  0-44-61-54-49-47-53-50-41-44-43-41-37-29-19 -9 -1  0  0  0  0  0  0  0  0
30      0  0  0  0  0  0  0-46-53-56-72-70-73-68-61-61-60-56-49-41-31-25 -1  0  0  0  0  0  0  0  0
31      0  0  0  0  0  0  0  0  0  0-96-95-94-87-81-80-79-73-62-55-45-43  0  0  0  0  0  0  0  0  0
```

Figure B-4 "Coma" Output Map

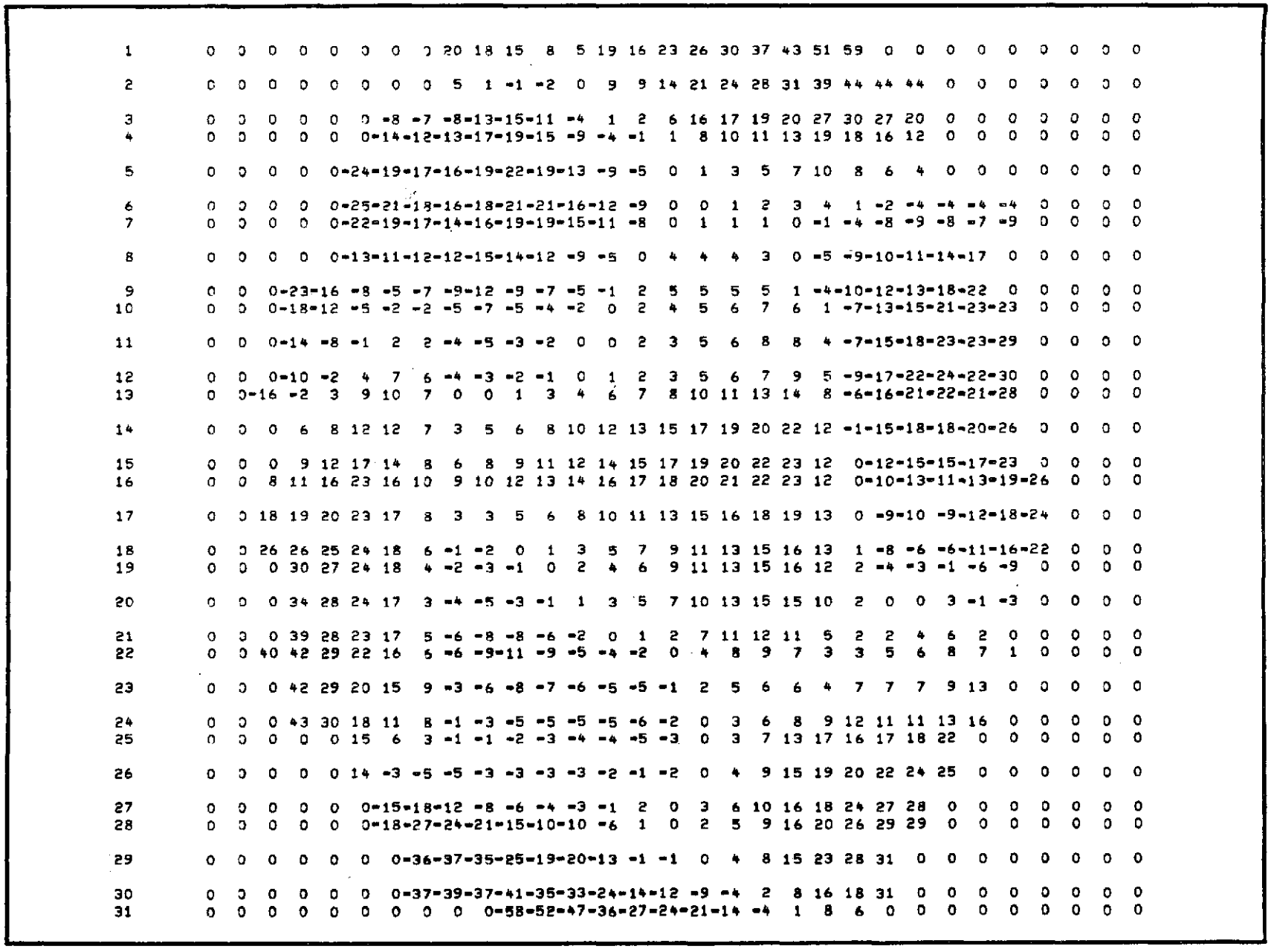

```
 1     0  0  0  0  0  0  0  0 20 18 15  8  5 19 16 23 26 30 37 43 51 59  0  0  0  0  0  0  0  0  0
 2     0  0  0  0  0  0  0  0  5  1 -1 -2  0  9  9 14 21 24 28 31 39 44 44 44  0  0  0  0  0  0  0
 3     0  0  0  0  0  0 -8 -7 -8-13-15-11 -4  1  2  6 16 17 19 20 27 30 27 20  0  0  0  0  0  0  0
 4     0  0  0  0  0  0-14-12-13-17-19-15 -9 -4 -1  1  8 10 11 13 19 18 16 12  0  0  0  0  0  0  0
 5     0  0  0  0  0-24-19-17-16-19-22-19-13 -9 -5  0  1  3  5  7 10  8  6  4  0  0  0  0  0  0  0
 6     0  0  0  0  0-25-21-18-16-18-21-21-16-12 -9  0  0  1  2  3  4  1 -2 -4 -4 -4 -4  0  0  0  0
 7     0  0  0  0  0-22-19-17-14-16-19-19-15-11 -8  0  1  1  1  0 -1 -4 -8 -9 -8 -7 -9  0  0  0  0
 8     0  0  0  0  0-13-11-12-12-15-14-12 -9 -5  0  4  4  4  3  0 -5 -9-10-11-14-17  0  0  0  0  0
 9     0  0  0-23-16 -8 -5 -7 -9-12 -9 -7 -5 -1  2  5  5  5  5  1 -4-10-12-13-18-22  0  0  0  0  0
10     0  0  0-18-12 -5 -2 -2 -5 -7 -5 -4 -2  0  2  4  5  6  7  6  1 -7-13-15-21-23-23  0  0  0  0
11     0  0  0-14 -8 -1  2  2 -4 -5 -3 -2  0  0  2  3  5  6  8  8  4 -7-15-18-23-23-29  0  0  0  0
12     0  0  0-10 -2  4  7  6 -4 -3 -2 -1  0  1  2  3  5  6  7  9  5 -9-17-22-24-22-30  0  0  0  0
13     0  0-16 -2  3  9 10  7  0  0  1  3  4  6  7  8 10 11 13 14  8 -6-16-21-22-21-28  0  0  0  0
14     0  0  0  6  8 12 12  7  3  5  6  8 10 12 13 15 17 19 20 22 12 -1-15-18-18-20-26  0  0  0  0
15     0  0  0  9 12 17 14  8  6  8  9 11 12 14 15 17 19 20 22 23 12  0-12-15-15-17-23  0  0  0  0
16     0  0  8 11 16 23 16 10  9 10 12 13 14 16 17 18 20 21 22 23 12  0-10-13-11-13-19-26  0  0  0
17     0  0 18 19 20 23 17  8  3  3  5  6  8 10 11 13 15 16 18 19 13  0 -9-10 -9-12-18-24  0  0  0
18     0  0 26 26 25 24 18  6 -1 -2  0  1  3  5  7  9 11 13 15 16 13  1 -8 -6 -6-11-16-22  0  0  0
19     0  0  0 30 27 24 18  4 -2 -3 -1  0  2  4  6  9 11 13 15 16 12  2 -4 -3 -1 -6 -9  0  0  0  0
20     0  0  0 34 28 24 17  3 -4 -5 -3 -1  1  3  5  7 10 13 15 15 10  2  0  0  3 -1 -3  0  0  0  0
21     0  0  0 39 28 23 17  5 -6 -8 -8 -6 -2  0  1  2  7 11 12 11  5  2  2  4  6  2  0  0  0  0  0
22     0  0 40 42 29 22 16  6 -6 -9-11 -9 -5 -4 -2  0  4  8  9  7  3  3  5  6  8  7  1  0  0  0  0
23     0  0  0 42 29 20 15  9 -3 -6 -8 -7 -6 -5 -5 -1  2  5  6  6  4  7  7  7  9 13  0  0  0  0  0
24     0  0  0 43 30 18 11  8 -1 -3 -5 -5 -5 -5 -6 -2  0  3  6  8  9 12 11 11 13 16  0  0  0  0  0
25     0  0  0  0  0 15  6  3 -1 -1 -2 -3 -4 -4 -5 -3  0  3  7 13 17 16 17 18 22  0  0  0  0  0  0
26     0  0  0  0  0 14 -3 -5 -5 -3 -3 -3 -3 -2 -1 -2  0  4  9 15 19 20 22 24 25  0  0  0  0  0  0
27     0  0  0  0  0  0-15-18-12 -8 -6 -4 -3 -1  2  0  3  6 10 16 18 24 27 28  0  0  0  0  0  0  0
28     0  0  0  0  0  0-18-27-24-21-15-10-10 -6  1  0  2  5  9 16 20 26 29 29  0  0  0  0  0  0  0
29     0  0  0  0  0  0  0-36-37-35-25-19-20-13 -1 -1  0  4  8 15 23 28 31  0  0  0  0  0  0  0  0
30     0  0  0  0  0  0  0-37-39-37-41-35-33-24-14-12 -9 -4  2  8 16 18 31  0  0  0  0  0  0  0  0
31     0  0  0  0  0  0  0  0  0  0-58-52-47-36-27-24-21-14 -4  1  8  6  0  0  0  0  0  0  0  0  0
```

Figure B-5 "Astigmatism" Output Map

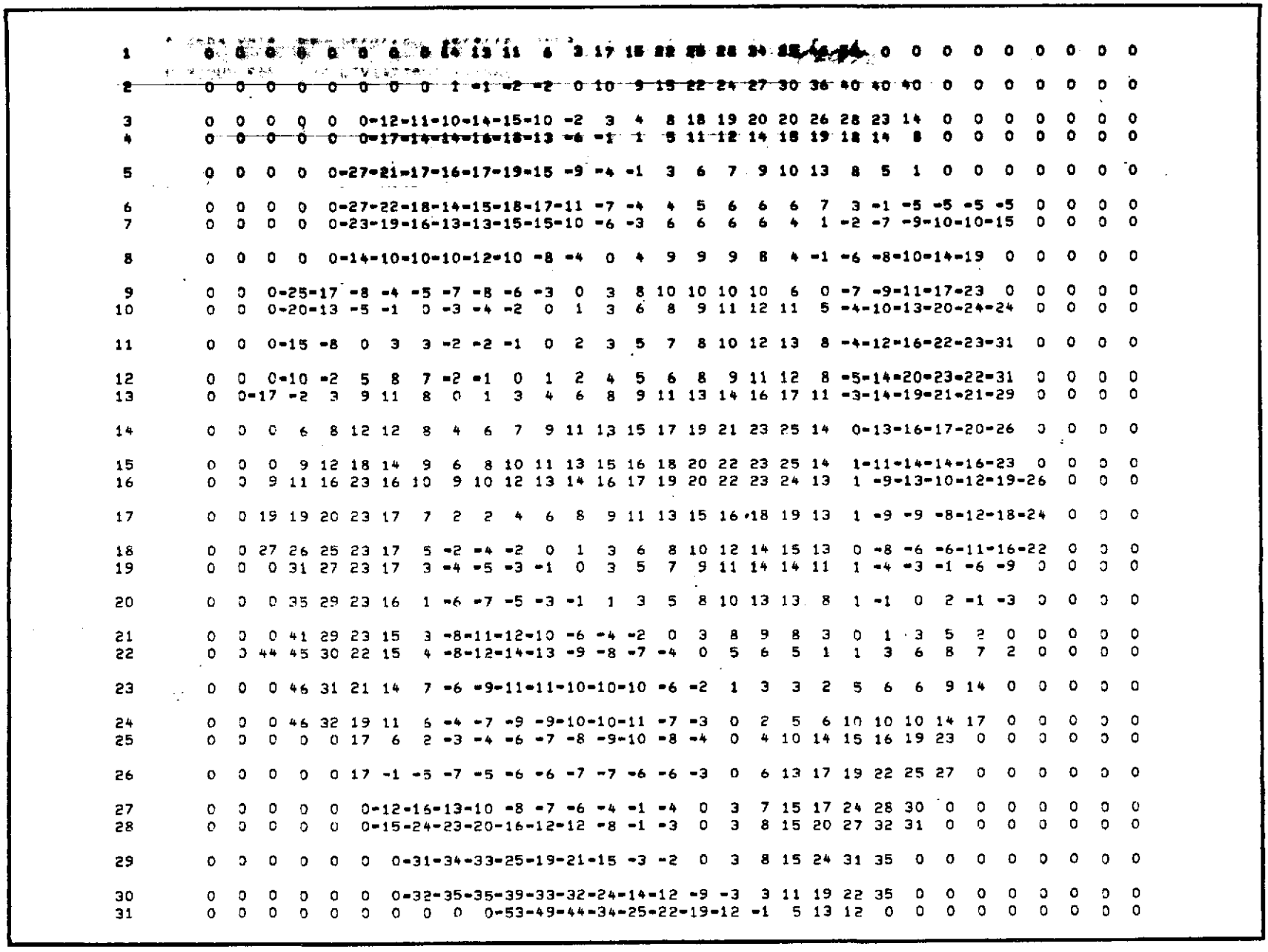

1	0	0	0	0	0	0	0	0	14	13	11	6	3	17	15	22	25	28	34	35	36	34	0	0	0	0	0	0	0	0	0
2	0	0	0	0	0	0	0	0	1	-1	-2	-2	0	10	9	15	22	24	27	30	36	40	40	40	0	0	0	0	0	0	0
3	0	0	0	0	0	0	-12	-11	-10	-14	-15	-10	-2	3	4	8	18	19	20	20	26	28	23	14	0	0	0	0	0	0	0
4	0	0	0	0	0	0	-17	-14	-14	-16	-18	-13	-6	-1	1	5	11	12	14	18	19	18	14	8	0	0	0	0	0	0	0
5	0	0	0	0	0	-27	-21	-17	-16	-17	-19	-15	-9	-4	-1	3	6	7	9	10	13	8	5	1	0	0	0	0	0	0	0
6	0	0	0	0	0	-27	-22	-18	-14	-15	-18	-17	-11	-7	-4	4	5	6	6	6	7	3	-1	-5	-5	-5	-5	0	0	0	0
7	0	0	0	0	0	-23	-19	-16	-13	-13	-15	-15	-10	-6	-3	6	6	6	6	4	1	-2	-7	-9	-10	-10	-15	0	0	0	0
8	0	0	0	0	0	-14	-10	-10	-10	-12	-10	-8	-4	0	4	9	9	9	8	4	-1	-6	-8	-10	-14	-19	0	0	0	0	0
9	0	0	0	-25	-17	-8	-4	-5	-7	-8	-6	-3	0	3	8	10	10	10	10	6	0	-7	-9	-11	-17	-23	0	0	0	0	0
10	0	0	0	-20	-13	-5	-1	0	-3	-4	-2	0	1	3	6	8	9	11	12	11	5	-4	-10	-13	-20	-24	-24	0	0	0	0
11	0	0	0	-15	-8	0	3	3	-2	-2	-1	0	2	3	5	7	8	10	12	13	8	-4	-12	-16	-22	-23	-31	0	0	0	0
12	0	0	0	-10	-2	5	8	7	-2	-1	0	1	2	4	5	6	8	9	11	12	8	-5	-14	-20	-23	-22	-31	0	0	0	0
13	0	0	-17	-2	3	9	11	8	0	1	3	4	6	8	9	11	13	14	16	17	11	-3	-14	-19	-21	-21	-29	0	0	0	0
14	0	0	0	6	8	12	12	8	4	6	7	9	11	13	15	17	19	21	23	25	14	0	-13	-16	-17	-20	-26	0	0	0	0
15	0	0	0	9	12	18	14	9	6	8	10	11	13	15	16	18	20	22	23	25	14	1	-11	-14	-14	-16	-23	0	0	0	0
16	0	0	9	11	16	23	16	10	9	10	12	13	14	16	17	19	20	22	23	24	13	1	-9	-13	-10	-12	-19	-26	0	0	0
17	0	0	19	19	20	23	17	7	2	2	4	6	8	9	11	13	15	16	18	19	13	1	-9	-9	-8	-12	-18	-24	0	0	0
18	0	0	27	26	25	23	17	5	-2	-4	-2	0	1	3	6	8	10	12	14	15	13	0	-8	-6	-6	-11	-16	-22	0	0	0
19	0	0	0	31	27	23	17	3	-4	-5	-3	-1	0	3	5	7	9	11	14	14	11	1	-4	-3	-1	-6	-9	0	0	0	0
20	0	0	0	35	29	23	16	1	-6	-7	-5	-3	-1	1	3	5	8	10	13	13	8	1	-1	0	2	-1	-3	0	0	0	0
21	0	0	0	41	29	23	15	3	-8	-11	-12	-10	-6	-4	-2	0	3	8	9	8	3	0	1	3	5	2	0	0	0	0	0
22	0	0	44	45	30	22	15	4	-8	-12	-14	-13	-9	-8	-7	-4	0	5	6	5	1	1	3	6	8	7	2	0	0	0	0
23	0	0	0	46	31	21	14	7	-6	-9	-11	-11	-10	-10	-10	-6	-2	1	3	3	2	5	6	6	9	14	0	0	0	0	0
24	0	0	0	46	32	19	11	6	-4	-7	-9	-9	-10	-10	-11	-7	-3	0	2	5	6	10	10	10	14	17	0	0	0	0	0
25	0	0	0	0	0	17	6	2	-3	-4	-6	-7	-8	-9	-10	-8	-4	0	4	10	14	15	16	19	23	0	0	0	0	0	0
26	0	0	0	0	0	17	-1	-5	-7	-5	-6	-6	-7	-7	-6	-6	-3	0	6	13	17	19	22	25	27	0	0	0	0	0	0
27	0	0	0	0	0	0	-12	-16	-13	-10	-8	-7	-6	-4	-1	-4	0	3	7	15	17	24	28	30	0	0	0	0	0	0	0
28	0	0	0	0	0	0	-15	-24	-23	-20	-16	-12	-12	-8	-1	-3	0	3	8	15	20	27	32	31	0	0	0	0	0	0	0
29	0	0	0	0	0	0	0	-31	-34	-33	-25	-19	-21	-15	-3	-2	0	3	8	15	24	31	35	0	0	0	0	0	0	0	0
30	0	0	0	0	0	0	0	-32	-35	-35	-39	-33	-32	-24	-14	-12	-9	-3	3	11	19	22	35	0	0	0	0	0	0	0	0
31	0	0	0	0	0	0	0	0	0	0	-53	-49	-44	-34	-25	-22	-19	-12	-1	5	13	12	0	0	0	0	0	0	0	0	0

Figure B-6 "Astigmatism/Coma" Output Map

Appendix C
VIBRATION TESTS OF TEST SITE

This work was done by Messrs. Clark and Sensmeier of MSFC. A copy of the cover letter of their report follows. They surveyed two possible test sites at BBRC and selected one on the basis of seismic and acoustical levels found. The complete report, including tracings, is available on request.

NATIONAL AERONAUTICS AND SPACE ADMINISTRATION
GEORGE C. MARSHALL SPACE FLIGHT CENTER
MARSHALL SPACE FLIGHT CENTER, ALABAMA 35812

REPLY TO ATTN OF: S&E-ASTR-GC

November 4, 1972

TO: S&E-ASTR-GCI/Mr. J. D. Johnston

FROM: S&E-ASTR-GCI/Mr. Clark
Mr. Sensmeier

SUBJECT: Trip Report

Date & Place of Visit: Ball Brothers Research Corporation (BBRC)
Boulder, Colorado
September 20-29, 1972

Purpose: This trip was made at the request of Mr. Max Nein (PD-MP-A) for the purpose of conducting floor stability tests necessary for determining the optimum photoheliograph test site.

Contacts:

a.	John Reach	BBRC	Photoheliograph Project Manager
b.	Art Olsen	BBRC	Photoheliograph Project Engineer
c.	Albert Franks	BBRC	
d.	Max Nein	NASA	PD-MP-A
e.	Charles Wyman	NASA	S&E-ASTR-RP

The photoheliograph built and to be tested by Ball Brothers Research Corporation is to be moved at a later date to the Solar Observatory on Big Bear Lake in California. This effort is for the purpose of solar information correlation between this photoheliograph and the experiments on the ATM Skylab satellites.

The following is a list of equipment used in determining the optimum photoheliograph test site.

a. Two Gulton $\pm$ 0.1G accelerometers set in the horizontal plane (one E-W, one N-S). The outputs of these sensors were recorded on a multichannel Sanborn recorder.

b. One Endevco, model 2410, detector was mounted in the vertical axis and its output was recorded on a multichannel Sanborn recorder. The Endevco is designed to detect low amplitude, relatively low frequency vibrations.

c. Two Ideal Aero-Smith tiltmeters set in the horizontal plane (one E-W, one N-S). The outputs of these sensors were recorded on two single channel Mosley recorders.

d. A Minco temperature measuring device monitored ambient temperature and was recorded on a suitable chart recorder.

Discussion:

1. The first tests (see Figure 1B) were conducted in the southwest corner of the Thompson II Building (see Figure 1A). In Figure 2 the N-S Gulton shows about 6 mV which is 0.00024G. Figure 2, the E-W Gulton, shows about 5 mV which is 0.00020G. The Endevco unit was inoperative at this time. Figures 3 and 4 show the outputs of the N-S and E-W tiltmeters. These charts are pretty much self-explanatory. The big excursions are caused by foot traffic. This is very low frequency and shows the floor to be spongy. The spongy or flexing floor is believed to be caused by voids underneath the floor.

2. The second tests were conducted at the BBRC Integration and Test Building (see Figure 1A). The setup was essentially the same as in the Thompson II Building. The Endevco unit was working during these tests. In Figure 5 the Endevco chart shows about 11 mV which is 0.003146G. In Figure 6 the N-S Gulton shows about 7 mV which is 0.00028G. The E-W Gulton shows about 15 mV or 0.00060G. Figures 7 and 8 show the E-W Ideal Aero-Smith sensor outputs. Figure 7 shows foot traffic near the sensors and Figure 8 shows just background noise. Figures 9 and 10 show the same thing about the N-S sensor.

3. While tests were in progress at the Integration and Test Building (I&T), we had a meeting with BBRC personnel to discuss test data to date. During this meeting we decided that when tests were concluded at I&T Building, we would move back to Thompson II Building for more tests. For the second tests at Thomspon II, a 4000 lb vehicle would be parked in the southwest corner of the building. This vehicle would simulate the weight of the four-wheel trailer, vacuum chamber and the photo-heliograph.

4. With a typical test setup back at Thompson II, it can be seen that the loading of the floor made a significant difference. Figures 11 and 12 are the outputs of the Ideal Aero-Smith tiltmeters which show a much tighter envelope when compared with earlier tests (Figures 3 and 4). This and other data indicate that the loading of the floor made the floor much stiffer. Due to a malfunctioning Sanborn recorder, we had only one channel on which we recorded the output of the Endevco sensor. The Endévco shows in Figure 13 an output of about 5 mV which is about 0.001430G.

5. Figures 14A, 14B, 15A and 15B were recorded on a visicorder for comparison only.

6. From the above data it can be seen that the I&T Building has several times as much seismic disturbances as the Thompson II Building. The I&T Building also had significant acoustical noise levels. The acoustical problems are generated by such things as the heating and cooling system, a laminar flow clean room, power generators, shake table, walk-in test chambers and miscellaneous blowers and motors.

7. In a second meeting with BBRC personnel, we discussed all the above information and concluded that the Thomspon II Building would be the test site for the photoheliograph. The times for conducting tests could be either at night or on weekends.

Summary:

For the testing of the photoheliograph at Ball Brothers Research Corporation two sites were evaluated, one was the Thompson II Building, the other was BBRC I&T Building.

The Thompson II Building was selected as the test site based on the following:

a. Seismic disturbances at Thomspon II were less than those measured at the I&T Building.

b. Acoustical problems at Thompson II were small and could be controlled.

c. Acoustical levels in the I&T Building were significantly high and not much can be done about it.

d. The Thompson II Building floor was obviously more flexible than the I&T Building floor as shown by foot traffic recordings in Figures 3, 4, 7, 9, 11 and 12. This is of no consequence however since foot traffic can be eliminated.

Foot traffic it seems usually generates frequencies of about 0.2 Hz per second. What is significant is shown in Figure 8, which shows continuous undesirable frequencies that are impractical to eliminate.

G LEVELS AT TEST SITES

	N-S	E-W	Vert.
Integration and Test Building	0.000280G	0.000600G	0.003146G
Thompson II Building	0.000240G	0.000200G	0.001430G

K. Clark

G. L. Sensmeier

cc:
S&E-ASTR-G/Mr. Mandel/Dr. Doane
S&E-ASTR-GC/Mr. Broussard/Mr. Morgan
S&E-ASTR-GCS/Mr. Walls/Mr. Kimmons
S&E-ASTR-RP/Mr. Wyman
PD-MP-A/Mr. Nein

~~NOTE:~~ Charts will ~~be forwarded at a later date because originals were~~ damaged in Reproduction.